

KEK-TH-576
 EPHOU-98-006
 hep-ph/9805448
 May 1998

Z' bosons in supersymmetric E_6 models confront electroweak data

Gi-Chol Cho^{1*}, Kaoru Hagiwara¹ and Yoshiaki Umeda^{1,2}

¹*Theory Group, KEK, Tsukuba, Ibaraki 305-0801, Japan*

²*Department of Physics, Hokkaido University, Sapporo 060-0810, Japan*

Abstract

We study constraints on additional Z' bosons predicted in the supersymmetric (SUSY) E_6 models by using the updated results of electroweak experiments – Z -pole experiments, m_W measurements and low-energy neutral current (LENC) experiments. We find that the effects of Z - Z' mixing are parametrized by (i) a tree-level contribution to the T -parameter, (ii) the effective Z - Z' mass mixing angle $\bar{\xi}$. In addition, the effect of the direct exchange of the heavier mass eigenstate Z_2 in the LENC processes is parametrized by (iii) a contact term $g_E^2/c_\chi^2 m_{Z_2}^2$. We give the theoretical predictions for the observables in the electroweak experiments together with the standard model radiative corrections. Constraints on T_{new} and $\bar{\xi}$ from the Z -pole and m_W experiments and those on $g_E^2/c_\chi^2 m_{Z_2}^2$ from the LENC experiments are separately shown. Impacts of the kinetic mixing between the $U(1)_Y$ and $U(1)'$ gauge bosons on the χ^2 -analysis are studied. We show the 95% CL lower mass limit of Z_2 as a function of the effective Z - Z' mixing parameter ζ , a combination of the mass and kinetic mixings. Theoretical prediction on ζ and g_E is found for the χ, ψ, η and ν models by assuming the minimal particle content of the SUSY E_6 models. In a certain region of the parameter space, the Z_2 boson mass in the detectable range of LHC is still allowed.

PACS: 12.10.Kt; 12.15.Lk; 12.60.Cn

Keywords: Supersymmetric E_6 models; Z' boson

*Research Fellow of the Japan Society for the Promotion of Science

1 Introduction

Although the minimal Standard Model (SM) agrees well with current electroweak experiments [1], it is important to examine consequences of new physics models beyond the SM at current or future collider experiments. One of the simplest extensions of the SM is to introduce an additional U(1) gauge symmetry, U(1)', whose breaking scale is close to the electroweak scale. The U(1)' symmetry is predicted in a certain class of grand unified theories (GUTs) with gauge group whose rank is higher than that of the SM. In general, the additional U(1)' gauge boson Z' can mix with the hypercharge U(1)_Y gauge boson through the kinetic term at above the electroweak scale, and also it can mix with the SM Z boson after the electroweak symmetry is spontaneously broken. Through those mixings, the Z' boson can affect the electroweak observables at the Z -pole and the W boson mass m_W . Both the Z - Z' mixing and the direct Z' contribution can affect neutral current experiments off the Z -pole. The presence of an additional Z' boson can be explored directly at $p\bar{p}$ collider experiments.

The supersymmetric (SUSY) E_6 models are the promising candidates which predict an additional Z' boson at the weak scale (for a review, see [2]). The gauge group E_6 can arise from the perturbative heterotic string theory as a consequence of its compactification. In the E_6 models, the SM matter fields in each generation are embedded into its fundamental representation **27** that also contains several exotic matter fields – two SM singlets, a pair of weak doublets and color triplets. Because E_6 is a rank-six group, it can have two extra U(1) factors besides the SM gauge group. A superposition of the two extra U(1) groups may survive as the U(1)' gauge symmetry at the GUT scale. The U(1)' symmetry may break spontaneously at the weak scale through the radiative corrections to the mass term of the SM singlet scalar field [3].

In this paper, we study constraints on the Z' bosons predicted in the SUSY E_6 models. Although there are several previous works [4, 5, 6, 7, 8], we would like to update their studies by using the recent results of electroweak experiments, and by allowing for an arbitrary kinetic mixing [9, 10, 11] between the Z' boson and the hypercharge B boson. In our study, we use the results of Z -pole experiments at LEP1 and SLC, and the m_W measurements at Tevatron and LEP2 which were reported at the summer conferences in 1997 [1]. We also study the constraints from low-energy neutral current (LENC) experiments: lepton-quark, lepton-lepton scattering experiments and atomic parity violation measurements.

We find that the lower mass limit of the heavier mass eigenstate Z_2 is obtained as a function of the effective Z - Z' mixing term ζ , which is a combination of the mass and kinetic mixings. In principle, ζ is calculable, together with the gauge coupling g_E , once the particle spectrum of the E_6 model is specified. We show the theoretical prediction for ζ and g_E in the SUSY E_6 models by assuming the minimal particle content which satisfies the anomaly free condition and the gauge coupling unification. For those models, the electroweak data give stringent lower mass bound on the Z_2 boson.

This paper is organized as follows. In the next section, we briefly review the additional Z' boson in the SUSY E_6 models and the generic feature of Z - Z' mixing in order to fix our notation. We show that the effects of Z - Z' mixing and direct Z' boson contribution are parametrized by the following three terms: (i) a tree-level contribution to the T parameter [12], T_{new} , (ii) the effective Z - Z' mass mixing angle $\bar{\xi}$ and (iii) a contact term $g_E^2/c_\chi^2 m_{Z_2}^2$ which appears in the low-energy processes. In Sec. 3, we collect the latest results of electroweak experiments. There, the theoretical predictions for the electroweak observables are shown together with the SM radiative corrections. In Sec. 4, we show constraints on the Z' bosons from the electroweak data. The presence of non-zero kinetic mixing between the $U(1)_Y$ and $U(1)'$ gauge bosons modifies the couplings between the Z' boson and the SM fermions. We discuss impacts of the kinetic mixing term on the χ^2 -analysis. The 95% CL lower mass limit of the heavier mass eigenstate Z_2 is given as a function of the effective Z - Z' mixing parameter ζ . The ζ -independent constraints from the low-energy experiments and those from the direct search experiments at Tevatron are also discussed. In Sec. 5, we find the theoretical prediction for ζ in some SUSY E_6 models (χ, ψ, η, ν) by assuming the minimal particle content. Stringent Z_2 boson mass bounds are found for most models. Sec. 6 summarizes our findings.

2 Z - Z' mixing in supersymmetric E_6 model

2.1 Z' boson in supersymmetric E_6 model

Since the rank of E_6 is six, it has two $U(1)$ factors besides the SM gauge group which arise from the following decompositions:

$$\begin{aligned} E_6 &\supset \text{SO}(10) \times U(1)_\psi \\ &\supset \text{SU}(5) \times U(1)_\chi \times U(1)_\psi. \end{aligned} \tag{2.1}$$

An additional Z' boson in the electroweak scale can be parametrized as a linear combination of the $U(1)_\psi$ gauge boson Z_ψ and the $U(1)_\chi$ gauge boson Z_χ as [13]

$$Z' = Z_\chi \cos \beta_E + Z_\psi \sin \beta_E. \quad (2.2)$$

In this paper, we study the following four Z' models in some detail:

β_E		0	$\pi/2$	$\tan^{-1}(-\sqrt{5/3})$	$\tan^{-1}(\sqrt{15})$	(2.3)
model		χ	ψ	η	ν	

In the SUSY- E_6 models, each generation of the SM quarks and leptons is embedded into a **27** representation. In Table 1, we show all the matter fields contained in a **27** and their classification in $SO(10)$ and $SU(5)$. The $U(1)'$ charge assignment on the matter fields for each model is also given in the same table. The normalization of the $U(1)'$ charge follows that of the hypercharge. Besides the SM quarks and leptons, there are two SM singlets ν^c and S , a pair of weak doublets H_u and H_d , a pair of color triplets D and \bar{D} in each generation. The η -model arises when E_6 breaks into a rank-5 group directly in a specific compactification of the heterotic string theory [14]. In the ν -model, the right-handed neutrinos ν^c are gauge singlet [15] and can have large Majorana masses to realize the see-saw mechanism [16].

The $U(1)'$ symmetry breaking occurs if the scalar component of the SM singlet field develops the vacuum expectation value (VEV). It can be achieved at near the weak scale via radiative corrections to the mass term of the SM singlet scalar field. For example, the terms $SD\bar{D}$ and SH_uH_d appear in the $SU(3)_C \times SU(2)_L \times U(1)_Y \times U(1)'$ invariant superpotential. If the Yukawa couplings of the $SD\bar{D}$ term and/or SH_uH_d term are $O(1)$, the squared mass of the scalar component of S can become negative at the weak scale through the renormalization group equations (RGEs) with an appropriate boundary condition at the GUT scale. Recent studies of the radiative $U(1)'$ symmetry breaking can be found, *e.g.*, in ref. [3].

Several problems may arise in the E_6 models from view of low-energy phenomenology [2]. For example, the scalar components of extra colored triplets D, \bar{D} in **27** could mediate an instant proton decay. It should be forbidden by imposing a certain discrete symmetry on the general $SU(3)_C \times SU(2)_L \times U(1)_Y \times U(1)'$ invariant superpotential. Except for the ν -model [15], the large Majorana mass of ν^c is forbidden by the $U(1)'$ gauge symmetry, and the fine-tuning is needed to make the Dirac neutrino mass consistent with the observation. Further discussions can be found in ref. [2]. In the following, we assume that these requirements are satisfied

Table 1: The hypercharge Y and the $U(1)'$ charge Q_E of all the matter fields in a **27** for the χ, ψ, η and ν models. The classification of the fields in the $SO(10)$ and the $SU(5)$ groups is also shown. The value of $U(1)'$ charge follows the hypercharge normalization.

$SO(10)$	$SU(5)$	field	Y	$2\sqrt{6}Q_\chi$	$\sqrt{72/5}Q_\psi$	Q_η	Q_ν	
16	10	Q	$+\frac{1}{6}$	-1	$+1$	$-\frac{1}{3}$	$+\sqrt{\frac{1}{24}}$	
		u^c	$-\frac{2}{3}$	-1	$+1$	$-\frac{1}{3}$	$+\sqrt{\frac{1}{24}}$	
		e^c	$+1$	-1	$+1$	$-\frac{1}{3}$	$+\sqrt{\frac{1}{24}}$	
	5	L	$-\frac{1}{2}$	$+3$	$+1$	$+\frac{1}{6}$	$+\sqrt{\frac{1}{6}}$	
		d^c	$+\frac{1}{3}$	$+3$	$+1$	$+\frac{1}{6}$	$+\sqrt{\frac{1}{6}}$	
	1	ν^c	0	-5	$+1$	$-\frac{5}{6}$	0	
	10	5	H_u	$+\frac{1}{2}$	$+2$	-2	$+\frac{2}{3}$	$-\sqrt{\frac{1}{6}}$
			D	$-\frac{1}{3}$	$+2$	-2	$+\frac{2}{3}$	$-\sqrt{\frac{1}{6}}$
		5	H_d	$-\frac{1}{2}$	-2	-2	$+\frac{1}{6}$	$-\sqrt{\frac{3}{8}}$
\bar{D}			$+\frac{1}{3}$	-2	-2	$+\frac{1}{6}$	$-\sqrt{\frac{3}{8}}$	
1		S	0	0	4	$-\frac{5}{6}$	$\sqrt{\frac{25}{24}}$	

by an unknown mechanism. Moreover we assume that all the super-partners of the SM particles and the exotic matters do not affect the radiative corrections to the electroweak observables significantly, *i.e.*, they are assumed to be heavy enough to decouple from the weak boson mass scale.

2.2 Phenomenological consequences of Z - Z' mixing

If the SM Higgs field carries a non-trivial $U(1)'$ charge, its VEV induces the Z - Z' mass mixing. On the other hand, the kinetic mixing between the hypercharge gauge boson B and the $U(1)'$ gauge boson Z' can occur through the quantum effects below the GUT scale. After the electroweak symmetry is broken, the effective Lagrangian for the neutral gauge bosons in the $SU(2)_L \times U(1)_Y \times U(1)'$ theory is

given by [10]

$$\begin{aligned} \mathcal{L}_{gauge} = & -\frac{1}{4}Z^{\mu\nu}Z_{\mu\nu} - \frac{1}{4}Z'^{\mu\nu}Z'_{\mu\nu} - \frac{\sin\chi}{2}B^{\mu\nu}Z'_{\mu\nu} - \frac{1}{4}A^{0\mu\nu}A_{\mu\nu}^0 \\ & + m_{ZZ'}^2 Z^\mu Z'_\mu + \frac{1}{2}m_Z^2 Z^\mu Z_\mu + \frac{1}{2}m_{Z'}^2 Z'^\mu Z'_\mu, \end{aligned} \quad (2.4)$$

where $F^{\mu\nu}$ ($F = Z, Z', A^0, B$) represents the gauge field strength. The Z - Z' mass mixing and the kinetic mixing are characterized by $m_{ZZ'}^2$ and $\sin\chi$, respectively. In this basis, the interaction Lagrangian for the neutral current process is given as

$$\begin{aligned} \mathcal{L}_{NC} = & -\sum_{f,\alpha} \left\{ e Q_{f_\alpha} \bar{f}_\alpha \gamma^\mu f_\alpha A_\mu^0 + g_Z \bar{f}_\alpha \gamma^\mu (I_{f_L}^3 - Q_{f_\alpha} \sin^2 \theta_W) f_\alpha Z_\mu \right. \\ & \left. + g_E Q_E^{f_\alpha} \bar{f}_\alpha \gamma^\mu f_\alpha Z'_\mu \right\}, \end{aligned} \quad (2.5)$$

where $g_Z = g/\cos\theta_W = g_Y/\sin\theta_W$. The $U(1)'$ gauge coupling constant is denoted by g_E in the hypercharge normalization. The symbol f_α denotes the quarks or leptons with the chirality α ($\alpha = L$ or R). The third component of the weak isospin, the electric charge and the $U(1)'$ charge of f_α are given by $I_{f_L}^3$, Q_{f_α} and $Q_E^{f_\alpha}$, respectively. The $U(1)'$ charge of the quarks and leptons listed in Table 1 should be read as

$$\left. \begin{aligned} Q_E^Q &= Q_E^{uL} = Q_E^{dL}, & Q_E^L &= Q_E^{\nu L} = Q_E^{eL}, \\ Q_E^{f^c} &= -Q_E^{fR} \quad (f = e, u, d), \end{aligned} \right\}. \quad (2.6)$$

The mass eigenstates (Z_1, Z_2, A) is obtained by the following transformation;

$$\begin{pmatrix} Z \\ Z' \\ A^0 \end{pmatrix} = \begin{pmatrix} \cos\xi + \sin\xi \sin\theta_W \tan\chi & -\sin\xi + \cos\xi \sin\theta_W \tan\chi & 0 \\ \sin\xi/\cos\chi & \cos\xi/\cos\chi & 0 \\ -\sin\xi \cos\theta_W \tan\chi & -\cos\xi \cos\theta_W \tan\chi & 1 \end{pmatrix} \begin{pmatrix} Z_1 \\ Z_2 \\ A \end{pmatrix}. \quad (2.7)$$

Here the mixing angle ξ is given by

$$\tan 2\xi = \frac{-2c_\chi(m_{ZZ'}^2 + s_W s_\chi m_Z^2)}{m_{Z'}^2 - (c_\chi^2 - s_W^2 s_\chi^2)m_Z^2 + 2s_W s_\chi m_{ZZ'}^2}, \quad (2.8)$$

with the short-hand notation, $c_\chi = \cos\chi$, $s_\chi = \sin\chi$ and $s_W = \sin\theta_W$. The physical masses m_{Z_1} and m_{Z_2} ($m_{Z_1} < m_{Z_2}$) are given as follows;

$$m_{Z_1}^2 = m_Z^2 (c_\xi + s_\xi s_W t_\chi)^2 + m_{Z'}^2 \left(\frac{s_\xi}{c_\chi} \right)^2 + 2m_{ZZ'}^2 \frac{s_\xi}{c_\chi} (c_\xi + s_\xi s_W t_\chi), \quad (2.9a)$$

$$m_{Z_2}^2 = m_Z^2 (c_\xi s_W t_\chi - s_\xi)^2 + m_{Z'}^2 \left(\frac{c_\xi}{c_\chi} \right)^2 + 2m_{ZZ'}^2 \frac{c_\xi}{c_\chi} (c_\xi s_W t_\chi - s_\xi), \quad (2.9b)$$

where $c_\xi = \cos \xi$, $s_\xi = \sin \xi$ and $t_\chi = \tan \chi$. The lighter mass eigenstate Z_1 should be identified with the observed Z boson at LEP1 or SLC. The excellent agreement between the current experimental results and the SM predictions at the quantum level implies that the mixing angle ξ have to be small. In the limit of small ξ , the interaction Lagrangians for the processes $Z_{1,2} \rightarrow f_\alpha \bar{f}_\alpha$ are expressed as

$$\mathcal{L}_{Z_1} = - \sum_{f,\alpha} g_Z \bar{f}_\alpha \gamma^\mu \left[\left(I_{fL}^3 - Q_{f_\alpha} \sin^2 \theta_W \right) + \tilde{Q}_E^{f_\alpha} \bar{\xi} \right] f_\alpha Z_{1\mu}, \quad (2.10a)$$

$$\mathcal{L}_{Z_2} = - \sum_{f,\alpha} \frac{g_E}{c_\chi} \bar{f}_\alpha \gamma^\mu \left[\tilde{Q}_E^{f_\alpha} - \left(I_{fL}^3 - Q_{f_\alpha} \sin^2 \theta_W \right) \frac{g_Z c_\chi \xi}{g_E} \right] f_\alpha Z_{2\mu}, \quad (2.10b)$$

where the effective mixing angle $\bar{\xi}$ in eq. (2.10a) is given as

$$\bar{\xi} = \frac{g_E}{g_Z \cos \chi} \xi. \quad (2.11)$$

In eq. (2.10), the effective U(1)' charge $\tilde{Q}_E^{f_\alpha}$ is introduced as a combination of $Q_E^{f_\alpha}$ and the hypercharge Y_{f_α} :

$$\tilde{Q}_E^{f_\alpha} \equiv Q_E^{f_\alpha} + Y_{f_\alpha} \delta, \quad (2.12a)$$

$$\delta \equiv - \frac{g_Z}{g_E} s_W s_\chi, \quad (2.12b)$$

where the hypercharge Y_{f_α} should be read from Table 1 in the same manner with $Q_E^{f_\alpha}$ (see, eq. (2.6)). As a notable example, one can see from Table 1 that the effective charge $\tilde{Q}_E^{f_\alpha}$ of the leptons (L and e^c) disappears in the η -model if δ is taken to be 1/3 [10].

Now, due to the Z - Z' mixing, the observed Z boson mass m_{Z_1} at LEP1 or SLC is shifted from the SM Z boson mass m_Z :

$$\Delta m^2 \equiv m_{Z_1}^2 - m_Z^2 \leq 0. \quad (2.13)$$

The presence of the mass shift affects the T -parameter [12] at tree level. Following the notation of ref. [17], the T -parameter is expressed in terms of the effective form factors $\bar{g}_Z^2(0)$, $\bar{g}_W^2(0)$ and the fine structure constant α :

$$\alpha T \equiv 1 - \frac{\bar{g}_W^2(0)}{m_W^2} \frac{m_{Z_1}^2}{\bar{g}_Z^2(0)} \quad (2.14a)$$

$$= \alpha (T_{\text{SM}} + T_{\text{new}}), \quad (2.14b)$$

where T_{SM} and the new physics contribution T_{new} are given by:

$$\alpha T_{\text{SM}} = 1 - \frac{\bar{g}_W^2(0)}{m_W^2} \frac{m_Z^2}{\bar{g}_Z^2(0)}, \quad (2.15a)$$

$$\alpha T_{\text{new}} = - \frac{\Delta m^2}{m_{Z_1}^2} \geq 0. \quad (2.15b)$$

It is worth noting that the sign of T_{new} is always positive. The effects of the Z - Z' mixing in the Z -pole experiments have hence been parametrized by the effective mixing angle $\bar{\xi}$ and the positive parameter T_{new} .

We note here that we retain the kinetic mixing term δ as a part of the effective Z_1 coupling $\tilde{Q}_E^{f\alpha}$ in eq. (2.12a). As shown in refs. [10, 11, 18], the kinetic mixing term δ can be absorbed into a further redefinition of S and T . Such reparametrization may be useful if the term $Y_f\delta$ in eq. (2.12a) is much larger than the Z' charge $Q_E^{f\alpha}$. In the E_6 models studied in this paper, we find no merit in absorbing the $Y_f\delta$ term because, the remaining $Q_E^{f\alpha}$ term is always significant. We therefore adopt $\tilde{Q}_E^{f\alpha}$ as the effective Z_1 couplings and T_{new} accounts only for the mass shift (2.13). All physical consequences such as the bounds on $\bar{\xi}$ and m_{Z_2} are of course independent of our choice of the parametrization.

The two parameters T_{new} and $\bar{\xi}$ are complicated functions of the parameters of the effective Lagrangian (2.4). In the small mixing limit, we find the following useful expressions

$$\bar{\xi} = -\left(\frac{g_E}{g_Z} \frac{m_Z}{m_{Z'}}\right)^2 \zeta \left[1 + O\left(\frac{m_Z^2}{m_{Z'}^2}\right)\right], \quad (2.16a)$$

$$\alpha T_{\text{new}} = \left(\frac{g_E}{g_Z} \frac{m_Z}{m_{Z'}}\right)^2 \zeta^2 \left[1 + O\left(\frac{m_Z^2}{m_{Z'}^2}\right)\right], \quad (2.16b)$$

where we introduced an effective mixing parameter ζ

$$\zeta = \frac{g_Z}{g_E} \frac{m_{Z'}^2}{m_Z^2} - \delta. \quad (2.17)$$

The Z - Z' mixing effect disappears at $\zeta = 0$. Stringent limits on $m_{Z'}$ and hence on m_{Z_2} can be obtained through the mixing effect if ζ is $O(1)$. We will show in Sec. 5 that ζ is calculable once the particle spectrum of the model is specified. The parameter ζ plays an essential role in the analysis of Z' models.

In the low-energy neutral current processes, effects of the exchange of the heavier mass eigenstate Z_2 can be detected. In the small $\bar{\xi}$ limit, they constrain the contact term $g_E^2/c_\chi^2 m_{Z_2}^2$.

3 Electroweak observables in the Z' model

In this section, we give the theoretical predictions for the electroweak observables which are used in our analysis. The experimental data of the Z -pole experiments and the W boson mass measurement [1] are summarized in Table 2. Those for the low-energy experiments [6] are listed in Table 3.

		pull = $\frac{\langle \text{data} \rangle - \text{best fit}}{\langle \text{error} \rangle}$					
		SM	χ	ψ	η	ν	η^*
Z-pole experiments							
m_Z (GeV)	91.1867 ± 0.0020						
Γ_Z (GeV)	2.4948 ± 0.0025	-0.8	-0.8	-0.6	-0.7	-0.7	-0.6
σ_h^0 (nb)	41.486 ± 0.053	0.3	0.6	0.6	0.3	0.6	0.2
R_ℓ	20.775 ± 0.027	0.9	0.8	0.7	0.9	0.7	1.1
$A_{FB}^{0,\ell}$	0.0171 ± 0.0010	0.8	0.8	0.7	0.7	0.8	0.7
A_τ	0.1411 ± 0.0064	-1.0	-1.0	-1.0	-1.0	-1.0	-1.0
A_e	0.1399 ± 0.0073	-1.1	-1.0	-1.1	-1.1	-1.1	-1.1
R_b	0.2170 ± 0.0009	1.4	1.4	1.5	1.4	1.4	0.6
R_c	0.1734 ± 0.0048	0.3	0.3	0.2	0.3	0.3	0.5
$A_{FB}^{0,b}$	0.0984 ± 0.0024	-2.1	-2.0	-2.1	-2.1	-2.1	-2.2
$A_{FB}^{0,c}$	0.0741 ± 0.0048	0.0	0.1	0.0	0.0	0.0	-0.1
A_{LR}^0	0.1547 ± 0.0032	2.2	2.3	2.2	2.2	2.2	2.2
A_b	0.900 ± 0.050	-0.7	-0.7	-0.7	-0.7	-0.7	-0.7
A_c	0.650 ± 0.058	-0.3	-0.3	-0.3	-0.3	-0.3	-0.4
W-mass measurement							
m_W (GeV)	80.43 ± 0.084	0.5	0.5	0.5	0.5	0.5	0.5
χ_{\min}^2 and d.o.f.							
χ_{\min}^2		16.9	16.7	16.7	16.9	16.6	16.1
d.o.f.		14	12	12	12	12	12
parameters	constraints	best fit values					
m_t (GeV)	175.6 ± 5.5	172.4	173.1	172.8	172.3	172.9	172.9
$\alpha_s(m_{Z_1})$	0.118 ± 0.003	0.1185	0.1179	0.1180	0.1185	0.1179	0.1192
$1/\bar{\alpha}(m_{Z_1}^2)$	128.75 ± 0.09	128.75	128.76	128.74	128.74	128.75	128.74
T_{new}	—	—	0	0	0	0	0
$\bar{\xi}$	—	—	0.0002	0.0002	-0.0001	0.0002	0.0027

Table 2: Summary of electroweak measurements for the Z-pole experiments and the m_W measurement [1]. The best fits to all the data in this Table are found by allowing the five parameters $m_t, \alpha_s(m_{Z_1}), \bar{\alpha}(m_{Z_1}^2), T_{\text{new}}$ and $\bar{\xi}$ to vary freely under the constraints $m_t = 175.6 \pm 5.5$ GeV [19], $\alpha_s(m_{Z_1}) = 0.118 \pm 0.003$ [13], $1/\bar{\alpha}(m_{Z_1}^2) = 128.75 \pm 0.09$ [21], $T_{\text{new}} \geq 0$ and $m_H = 100$ GeV. The results for the χ, ψ, η and ν models are obtained by setting $\delta = 0$. The symbol η^* denotes the leptophobic η -model where δ is taken to be $\delta = 1/3$.

		pull = $\frac{\langle \text{data} \rangle - \text{best fit}}{\langle \text{error} \rangle}$					
		SM	χ	ψ	η	ν	η^*
LENC experiments							
A_{SLAC}	0.80 ± 0.058	1.0	1.0	1.0	1.0	1.0	0.9
A_{CERN}	-1.57 ± 0.38	-0.4	-0.4	-0.4	-0.4	-0.4	-0.4
A_{Bates}	-0.137 ± 0.033	0.5	0.4	0.4	0.4	0.4	0.5
A_{Mainz}	-0.94 ± 0.19	-0.3	-0.3	-0.3	-0.4	-0.3	-0.3
$Q_W(^{133}\text{C}_s)$	-72.08 ± 0.92	1.0	-0.2	1.0	0.2	-0.1	1.3
K_{FH}	0.3247 ± 0.0040	-1.5	-1.4	-1.5	-1.5	-1.4	-1.4
K_{CCFR}	0.5820 ± 0.0049	-0.5	-0.4	-0.3	-0.4	-0.4	-0.5
$g_{LL}^{\nu_\mu e}$	-0.269 ± 0.011	0.4	0.1	0.1	0.5	0.1	0.4
$g_{LR}^{\nu_\mu e}$	0.234 ± 0.011	0.1	0.0	0.4	0.2	0.2	0.1
χ_{\min}^2 and d.o.f.							
χ_{\min}^2		22.0	20.2	21.5	21.2	20.4	21.7
d.o.f.		23	20	20	20	20	21
parameters	constraints	best fit values					
m_t (GeV)	175.6 ± 5.5	171.6	172.3	172.1	171.5	172.3	172.0
$\alpha_s(m_{Z_1})$	0.118 ± 0.003	0.1185	0.1181	0.1181	0.1185	0.1181	0.1189
$1/\bar{\alpha}(m_{Z_1})$	128.75 ± 0.09	128.75	128.75	128.75	128.73	128.75	128.75
T_{new}		—	0.0	0.0	0.0	0.0	0.0
$\bar{\xi}$		—	0.0001	0.0002	-0.0003	0.0001	0.0016
$g_E^2/c_\chi^2 m_{Z_E}^2$		—	0.279	1.771	-0.646	0.668	—

Table 3: Summary of measurements for the low-energy neutral current experiments [6]. The best fits are found by using all the electroweak data of Table 2 and those in this Table. The results for the χ , ψ , η and ν models are obtained by setting $\delta = 0$. The symbol η^* denotes the leptophobic η -model where δ is taken to be $\delta = 1/3$.

3.1 Observables in Z -pole experiments

The decay amplitude for the process $Z_1 \rightarrow f_\alpha \bar{f}_\alpha$ is written as

$$T(Z_1 \rightarrow f_\alpha \bar{f}_\alpha) = M_\alpha^f \epsilon_{Z_1} \cdot J_{f_\alpha}, \quad (3.1)$$

where $\epsilon_{Z_1}^\mu$ is the polarization vector of the Z_1 boson and $J_{f_\alpha}^\mu = \bar{f}_\alpha \gamma^\mu f_\alpha$ is the fermion current without the coupling factors. The pseudo-observables of the Z -pole experiments are expressed in terms of the real scalar amplitudes M_α^f with the following normalization [1]

$$g_\alpha^f = \frac{M_\alpha^f}{\sqrt{4\sqrt{2}G_F m_{Z_1}^2}} \approx \frac{M_\alpha^f}{0.74070}. \quad (3.2)$$

Following our parametrization of the Z - Z' mixing in eq. (2.10a), the effective coupling g_α^f in the Z' models can be expressed as

$$g_\alpha^f = (g_\alpha^f)_{\text{SM}} + \tilde{Q}_E^{f\alpha} \bar{\xi}. \quad (3.3)$$

The SM predictions [17, 20] for the effective couplings $(g_\alpha^f)_{\text{SM}}$ can be parametrized as

$$(g_L^\nu)_{\text{SM}} = 0.50214 + 0.453 \Delta \bar{g}_Z^2, \quad (3.4a)$$

$$(g_L^e)_{\text{SM}} = -0.26941 - 0.244 \Delta \bar{g}_Z^2 + 1.001 \Delta \bar{s}^2, \quad (3.4b)$$

$$(g_R^e)_{\text{SM}} = 0.23201 + 0.208 \Delta \bar{g}_Z^2 + 1.001 \Delta \bar{s}^2, \quad (3.4c)$$

$$(g_L^u)_{\text{SM}} = 0.34694 + 0.314 \Delta \bar{g}_Z^2 - 0.668 \Delta \bar{s}^2, \quad (3.4d)$$

$$(g_R^u)_{\text{SM}} = -0.15466 - 0.139 \Delta \bar{g}_Z^2 - 0.668 \Delta \bar{s}^2, \quad (3.4e)$$

$$(g_L^d)_{\text{SM}} = -0.42451 - 0.383 \Delta \bar{g}_Z^2 + 0.334 \Delta \bar{s}^2, \quad (3.4f)$$

$$(g_R^d)_{\text{SM}} = 0.07732 + 0.069 \Delta \bar{g}_Z^2 + 0.334 \Delta \bar{s}^2, \quad (3.4g)$$

$$(g_L^b)_{\text{SM}} = -0.42109 - 0.383 \Delta \bar{g}_Z^2 + 0.334 \Delta \bar{s}^2 + 0.00043 x_t, \quad (3.4h)$$

where the SM radiative corrections are expressed in terms of the effective couplings $\Delta \bar{g}_Z^2$ and $\Delta \bar{s}^2$ [17, 20] and the top-quark mass dependence of the $Z b_L b_L$ vertex correction in $(g_L^b)_{\text{SM}}$ is parametrized by the parameter x_t

$$x_t \equiv \frac{m_t - 175 \text{ GeV}}{10 \text{ GeV}}. \quad (3.5)$$

The gauge boson propagator corrections, $\Delta \bar{g}_Z^2$ and $\Delta \bar{s}^2$, are defined as the shift in the effective couplings $\bar{g}_Z^2(m_{Z_1}^2)$ and $\bar{s}^2(m_{Z_1}^2)$ [17] from their SM reference values at

$m_t = 175$ GeV and $m_H = 100$ GeV. They can be expressed in terms of the S and T parameters as

$$\Delta\bar{g}_Z^2 = \bar{g}_Z^2(m_{Z_1}^2) - 0.55635 = 0.00412\Delta T + 0.00005[1 - (100 \text{ GeV}/m_H)^2], \quad (3.6a)$$

$$\Delta\bar{s}^2 = \bar{s}^2(m_{Z_1}^2) - 0.23035 = 0.00360\Delta S - 0.00241\Delta T - 0.00023x_\alpha, \quad (3.6b)$$

where the expansion parameter x_α is introduced to estimate the uncertainty of the hadronic contribution to the QED coupling $1/\bar{\alpha}(m_{Z_1}^2) = 128.75 \pm 0.09$ [21]:

$$x_\alpha \equiv \frac{1/\bar{\alpha}(m_{Z_1}^2) - 128.75}{0.09}. \quad (3.7)$$

Here, $\Delta S, \Delta T, \Delta U$ parameters are also measured from their SM reference values and they are given as the sum of the SM and the new physics contributions

$$\Delta S = \Delta S_{\text{SM}} + S_{\text{new}}, \quad \Delta T = \Delta T_{\text{SM}} + T_{\text{new}}, \quad \Delta U = \Delta U_{\text{SM}} + U_{\text{new}}. \quad (3.8)$$

The SM contributions can be parametrized as [20]

$$\Delta S_{\text{SM}} = -0.007x_t + 0.091x_H - 0.010x_H^2, \quad (3.9a)$$

$$\begin{aligned} \Delta T_{\text{SM}} = & (0.130 - 0.003x_H)x_t + 0.003x_t - 0.079x_H - 0.028x_H^2 \\ & + 0.0026x_H^3, \end{aligned} \quad (3.9b)$$

$$\Delta U_{\text{SM}} = 0.022x_t - 0.002x_H, \quad (3.9c)$$

where x_H is defined by

$$x_H \equiv \log(m_H/100 \text{ GeV}). \quad (3.10)$$

The pseudo-observables of the Z -pole experiments are given by using the above eight effective couplings g_α^f as follows. The partial width of Z_1 boson is given by

$$\Gamma_f = \frac{G_F m_{Z_1}^3}{3\sqrt{2}\pi} \left\{ |g_L^f + g_R^f|^2 \frac{C_{fV}}{2} + |g_L^f - g_R^f|^2 \frac{C_{fA}}{2} \right\} \left(1 + \frac{3}{4} Q_f^2 \frac{\bar{\alpha}(m_{Z_1}^2)}{\pi} \right), \quad (3.11)$$

where the factors C_{fV} and C_{fA} account for the finite mass corrections and the final state QCD corrections for quarks. Their numerical values are listed in Table 4. The α_s -dependence in C_{qV}, C_{qA} is parametrized in terms of the parameter x_s

$$x_s \equiv \frac{\alpha_s(m_{Z_1}) - 0.118}{0.003}. \quad (3.12)$$

The last term proportional to $\bar{\alpha}(m_{Z_1}^2)/\pi$ in eq. (3.11) accounts for the final state QED correction. The total decay width Γ_{Z_1} and the hadronic decay width Γ_h are

	C_{fV}	C_{fA}
u	$3.1166 + 0.0030x_s$	$3.1351 + 0.0040x_s$
$d = s$	$3.1166 + 0.0030x_s$	$3.0981 + 0.0021x_s$
c	$3.1167 + 0.0030x_s$	$3.1343 + 0.0041x_s$
b	$3.1185 + 0.0030x_s$	$3.0776 + 0.0030x_s$
ν	1	1
$e = \mu$	1	1
τ	1	0.9977

Table 4: Numerical values of factors C_{fV}, C_{fA} for quarks and leptons used in eq. (3.11). The finite mass corrections and the final state QCD corrections for quarks are taken into accounted.

given in terms of Γ_f :

$$\Gamma_{Z_1} = 3\Gamma_\nu + \Gamma_e + \Gamma_\mu + \Gamma_\tau + \Gamma_h, \quad (3.13a)$$

$$\Gamma_h = \Gamma_u + \Gamma_c + \Gamma_d + \Gamma_s + \Gamma_b. \quad (3.13b)$$

The ratios R_ℓ, R_c, R_b and the hadronic peak cross section σ_h^0 are given by:

$$R_\ell = \frac{\Gamma_h}{\Gamma_e}, \quad R_c = \frac{\Gamma_c}{\Gamma_h}, \quad R_b = \frac{\Gamma_b}{\Gamma_h}, \quad \sigma_h^0 = \frac{12\pi}{m_{Z_1}^2} \frac{\Gamma_e \Gamma_h}{\Gamma_{Z_1}^2}. \quad (3.14)$$

The left-right asymmetry parameter A^f is also given in terms of the effective couplings g_α^f as

$$A^f = \frac{(g_L^f)^2 - (g_R^f)^2}{(g_L^f)^2 + (g_R^f)^2}. \quad (3.15)$$

The forward-backward (FB) asymmetry $A_{FB}^{0,f}$ and the left-right (LR) asymmetry $A_{LR}^{0,f}$ are then given as follows:

$$A_{FB}^{0,f} = \frac{3}{4} A^e A^f, \quad (3.16a)$$

$$A_{LR}^{0,f} = A^f. \quad (3.16b)$$

3.2 W boson mass

The theoretical prediction of m_W can be parametrized as [17, 20]

$$m_W(\text{GeV}) = 80.402 - 0.288 \Delta S + 0.418 \Delta T + 0.337 \Delta U + 0.012 x_\alpha, \quad (3.17)$$

by using the same parameters, $\Delta S, \Delta T, \Delta U$ (3.8) and x_α (3.7).

3.3 Observables in low-energy experiments

In this subsection, we show the theoretical predictions for the electroweak observables in the low-energy neutral current experiments (LENC) — (i) polarization asymmetry of the charged lepton scattering off nucleus target (3.3.1–3.3.4), (ii) parity violation in cesium atom (3.3.5), (iii) inelastic ν_μ -scattering off nucleus target (3.3.6) and (iv) neutrino-electron scattering (3.3.7). The experimental data are summarized in Table 3. Theoretical expressions for the observables of (i) and (ii) are conveniently given in terms of the model-independent parameters C_{1q}, C_{2q} [22] and C_{3q} [6]. The ν_μ -scattering data (iii) and (iv) are expressed in terms of the parameters $g_{L\alpha}^{\nu\mu f}$. All the model-independent parameters can be expressed compactly in terms of the reduced helicity amplitudes $M_{\alpha\beta}^{ff'}$ [6, 17] of the process $f_\alpha f'_\beta \rightarrow f_\alpha f'_\beta$:

$$C_{1q} = \frac{1}{2\sqrt{2}G_F} (M_{LL}^{\ell q} + M_{LR}^{\ell q} - M_{RL}^{\ell q} - M_{RR}^{\ell q}), \quad (3.1a)$$

$$C_{2q} = \frac{1}{2\sqrt{2}G_F} (M_{LL}^{\ell q} - M_{LR}^{\ell q} + M_{RL}^{\ell q} - M_{RR}^{\ell q}), \quad (3.1b)$$

$$C_{3q} = \frac{1}{2\sqrt{2}G_F} (-M_{LL}^{\ell q} + M_{LR}^{\ell q} + M_{RL}^{\ell q} - M_{RR}^{\ell q}), \quad (3.1c)$$

$$g_{L\alpha}^{\nu\mu f} = \frac{1}{2\sqrt{2}G_F} (-M_{L\alpha}^{\nu\mu f}). \quad (3.1d)$$

Below, we divide these model-independent parameters into two pieces as

$$C_{iq} = (C_{iq})_{\text{SM}} + \Delta C_{iq}, \quad (3.2a)$$

$$g_{L\alpha}^{\nu\mu f} = (g_{L\alpha}^{\nu\mu f})_{\text{SM}} + \Delta g_{L\alpha}^{\nu\mu f}, \quad (3.2b)$$

where the first term in each equation is the SM contribution which is parametrized conveniently by ΔS and ΔT in ref. [6]. The terms ΔC_{iq} and $\Delta g_{L\alpha}^{\nu\mu f}$ represent the additional contributions from the Z - Z' mixing and the Z_2 exchange:

$$\Delta C_{1u} = (-0.19s_\beta - 0.15c_\beta + 0.65\delta)\bar{\xi} - \frac{g_E^2 (\tilde{Q}_E^L - \tilde{Q}_E^E)(\tilde{Q}_E^Q + \tilde{Q}_E^U)}{c_\chi^2 2\sqrt{2}G_F m_{Z_2}^2}, \quad (3.3a)$$

$$\Delta C_{1d} = (0.36s_\beta - 0.54c_\beta + 0.17\delta)\bar{\xi} - \frac{g_E^2 (\tilde{Q}_E^L - \tilde{Q}_E^E)(\tilde{Q}_E^Q + \tilde{Q}_E^D)}{c_\chi^2 2\sqrt{2}G_F m_{Z_2}^2}, \quad (3.3b)$$

$$\Delta C_{2u} = (0.02s_\beta - 0.84c_\beta + 1.48\delta)\bar{\xi} - \frac{g_E^2 (\tilde{Q}_E^L + \tilde{Q}_E^E)(\tilde{Q}_E^Q - \tilde{Q}_E^U)}{c_\chi^2 2\sqrt{2}G_F m_{Z_2}^2}, \quad (3.3c)$$

$$\Delta C_{2d} = (0.02s_\beta + 0.84c_\beta - 1.48\delta)\bar{\xi} - \frac{g_E^2 (\tilde{Q}_E^L + \tilde{Q}_E^E)(\tilde{Q}_E^Q - \tilde{Q}_E^D)}{c_\chi^2 2\sqrt{2}G_F m_{Z_2}^2}, \quad (3.3d)$$

$$\Delta C_{3u} = (-0.82c_\beta + 1.00\delta)\bar{\xi} - \frac{g_E^2}{c_\chi^2} \frac{(\tilde{Q}_E^L - \tilde{Q}_E^E)(\tilde{Q}_E^U - \tilde{Q}_E^Q)}{2\sqrt{2}G_F m_{Z_2}^2}, \quad (3.3e)$$

$$\Delta C_{3d} = (1.06s_\beta - 0.82c_\beta - 1.00\delta)\bar{\xi} - \frac{g_E^2}{c_\chi^2} \frac{(\tilde{Q}_E^L - \tilde{Q}_E^E)(\tilde{Q}_E^D - \tilde{Q}_E^Q)}{2\sqrt{2}G_F m_{Z_2}^2}, \quad (3.3f)$$

$$\Delta g_{LL}^{\nu u} = (0.44s_\beta + 0.22c_\beta - 0.18\delta)\bar{\xi} + \frac{g_E^2}{c_\chi^2} \frac{\tilde{Q}_E^L \tilde{Q}_E^Q}{2\sqrt{2}G_F m_{Z_2}^2}, \quad (3.3g)$$

$$\Delta g_{LR}^{\nu u} = (-0.35s_\beta + 0.01c_\beta + 0.82\delta)\bar{\xi} + \frac{g_E^2}{c_\chi^2} \frac{\tilde{Q}_E^L \tilde{Q}_E^U}{2\sqrt{2}G_F m_{Z_2}^2}, \quad (3.3h)$$

$$\Delta g_{LL}^{\nu d} = (0.04s_\beta - 0.72c_\beta + 0.59\delta)\bar{\xi} + \frac{g_E^2}{c_\chi^2} \frac{\tilde{Q}_E^L \tilde{Q}_E^Q}{2\sqrt{2}G_F m_{Z_2}^2}, \quad (3.3i)$$

$$\Delta g_{LR}^{\nu d} = (-0.22s_\beta - 0.52c_\beta - 0.41\delta)\bar{\xi} + \frac{g_E^2}{c_\chi^2} \frac{\tilde{Q}_E^L \tilde{Q}_E^D}{2\sqrt{2}G_F m_{Z_2}^2}, \quad (3.3j)$$

$$\Delta g_{LL}^{\nu e} = (0.12s_\beta + 0.28c_\beta - 0.23\delta)\bar{\xi} + \frac{g_E^2}{c_\chi^2} \frac{\tilde{Q}_E^L \tilde{Q}_E^L}{2\sqrt{2}G_F m_{Z_2}^2}, \quad (3.3k)$$

$$\Delta g_{LR}^{\nu e} = (-0.14s_\beta + 0.49c_\beta - 1.23\delta)\bar{\xi} + \frac{g_E^2}{c_\chi^2} \frac{\tilde{Q}_E^L \tilde{Q}_E^e}{2\sqrt{2}G_F m_{Z_2}^2}. \quad (3.3l)$$

where $c_\beta = \cos \beta_E$ and $s_\beta = \sin \beta_E$.

3.3.1 SLAC eD experiment

The parity asymmetry in the inelastic scattering of polarized electrons from the deuterium target was measured at SLAC [23]. The experiment constrains the parameters $2C_{1u} - C_{1d}$ and $2C_{2u} - C_{2d}$. The most stringent constraint shown in Table 3 is found for the following combination

$$A_{\text{SLAC}} = 2C_{1u} - C_{1d} + 0.206(2C_{2u} - C_{2d}) \quad (3.4a)$$

$$= 0.745 - 0.016 \Delta S + 0.016 \Delta T \\ + 2\Delta C_{1u} - \Delta C_{1d} + 0.206(2\Delta C_{2u} - \Delta C_{2d}), \quad (3.4b)$$

where the theoretical prediction [6] is evaluated at the mean momentum transfer $\langle Q^2 \rangle = 1.5 \text{ GeV}^2$.

3.3.2 CERN $\mu^\pm C$ experiment

The CERN $\mu^\pm C$ experiment [24] measured the charge and polarization asymmetry of deep-inelastic muon scattering off the ^{12}C target. The mean momentum transfer of the experiment may be estimated at $\langle Q^2 \rangle = 50 \text{ GeV}^2$ [25]. The experiment

constrains the parameters $2C_{2u}-C_{2d}$ and $2C_{3u}-C_{3d}$. The most stringent constraint is found for the following combination [6]

$$A_{\text{CERN}} = 2C_{3u} - C_{3d} + 0.777(2C_{2u} - C_{2d}) \quad (3.5a)$$

$$\begin{aligned} &= -1.42 - 0.016 \Delta S + 0.0006 \Delta T \\ &\quad + 2\Delta C_{3u} - \Delta C_{3d} + 0.777(2\Delta C_{2u} - \Delta C_{2d}). \end{aligned} \quad (3.5b)$$

3.3.3 Bates $e\text{C}$ experiment

The polarization asymmetry of the electron elastic scattering off the ^{12}C target was measured at Bates [26]. The experiment constrains the combination

$$A_{\text{Bates}} = C_{1u} + C_{1d} \quad (3.6a)$$

$$= -0.1520 - 0.0023 \Delta S + 0.0004 \Delta T + \Delta C_{1u} + \Delta C_{1d}, \quad (3.6b)$$

where the theoretical prediction [6] is evaluated at $\langle Q^2 \rangle = 0.0225 \text{ GeV}^2$.

3.3.4 Mainz $e\text{Be}$ experiment

The polarization asymmetry of electron quasi-elastic scattering off the ^9Be target was measured at Mainz [27]. The data shown in Table 3 is for the combination

$$A_{\text{Mainz}} = -2.73C_{1u} + 0.65C_{1d} - 2.19C_{2u} + 2.03C_{2d} \quad (3.7a)$$

$$\begin{aligned} &= -0.876 + 0.043\Delta S - 0.035\Delta T \\ &\quad - 2.73\Delta C_{1u} + 0.65\Delta C_{1d} - 2.19\Delta C_{2u} + 2.03\Delta C_{2d}, \end{aligned} \quad (3.7b)$$

where the theoretical prediction [6] is evaluated at $\langle Q^2 \rangle = 0.2025 \text{ GeV}^2$.

3.3.5 Atomic Parity Violation

The experimental results of parity violation in the atom are often given in terms of the weak charge $Q_W(A, Z)$ of nuclei. By using the model-independent parameter C_{1q} , the weak charge of a nuclei can be expressed as

$$Q_W(A, Z) = 2ZC_{1p} + 2(A - Z)C_{1n}. \quad (3.8)$$

By taking account of the long-distance photonic correction [28], we find C_{1p} and C_{1n} as

$$C_{1p} = 0.03601 - 0.00681\Delta S + 0.00477 \Delta T + 2\Delta C_{1u} + \Delta C_{1d}, \quad (3.9a)$$

$$C_{1n} = -0.49376 - 0.00366 \Delta T + \Delta C_{1u} + 2\Delta C_{1d}. \quad (3.9b)$$

The data for cesium atom $^{133}_{55}\text{Cs}$ [29, 30] is given in Table 3 and the theoretical prediction of the weak charge is found to be [6]

$$Q_W(^{133}_{55}\text{Cs}) = -73.07 - 0.749 \Delta S - 0.046 \Delta T + 376\Delta C_{1u} + 422\Delta C_{1d}. \quad (3.10)$$

3.3.6 Neutrino-quark scattering

For the ν_μ -quark scattering, the experimental results up to the year 1988 were summarized in ref. [31] in terms of the model-independent parameters $g_L^2, g_R^2, \delta_L^2, \delta_R^2$. The most stringent constraint on the result in ref. [31] is found for the following combination:

$$K_{\text{FH}} = g_L^2 + 0.879g_R^2 - 0.010\delta_L^2 - 0.043\delta_R^2. \quad (3.11)$$

More recent CCFR experiment at Tevatron measured the following combination [32]

$$K_{\text{CCFR}} = 1.7897g_L^2 + 1.1479g_R^2 - 0.0916\delta_L^2 - 0.0782\delta_R^2. \quad (3.12)$$

The data are shown in Table 3 and the SM predictions are calculated from our reduced amplitudes (3.1d) as follows [6, 17]

$$g_\alpha^2 = (g_{L\alpha}^{\nu_\mu u})^2 + (g_{L\alpha}^{\nu_\mu d})^2, \quad \delta_\alpha^2 = (g_{L\alpha}^{\nu_\mu u})^2 - (g_{L\alpha}^{\nu_\mu d})^2, \quad (3.13)$$

for $\alpha = L$ and R , respectively, where

$$g_{LL}^{\nu_\mu u} = 0.3468 - 0.0023\Delta S + 0.0041\Delta T, \quad (3.14a)$$

$$g_{LR}^{\nu_\mu u} = -0.1549 - 0.0023\Delta S + 0.0004\Delta T, \quad (3.14b)$$

$$g_{LL}^{\nu_\mu d} = -0.4299 + 0.0012\Delta S - 0.0039\Delta T, \quad (3.14c)$$

$$g_{LR}^{\nu_\mu d} = 0.0775 + 0.0012\Delta S - 0.0002\Delta T. \quad (3.14d)$$

The above predictions are obtained at the momentum transfer $\langle Q^2 \rangle = 35 \text{ GeV}^2$ relevant for the CCFR experiment [32]. The estimations are found to be valid [6] also for the data of ref. [31], whose typical scale is $\langle Q^2 \rangle = 20 \text{ GeV}^2$.

3.3.7 Neutrino-electron scattering

The ν_μ - e scattering experiments measure the neutral currents in a purely leptonic channel. The combined results [6, 33] are given in Table 3. The theoretical predictions

$$g_{LL}^{\nu_\mu e} = -0.273 + 0.0033\Delta S - 0.0042\Delta T + \Delta g_{LL}^{\nu_\mu e}, \quad (3.15a)$$

$$g_{LR}^{\nu_\mu e} = 0.233 + 0.0033\Delta S - 0.0006\Delta T + \Delta g_{LR}^{\nu_\mu e}, \quad (3.15b)$$

are evaluated at $\langle Q^2 \rangle = 2m_e E_\nu$ with $E_\nu = 25.7$ GeV for the CHARM-II experiment [33].

4 Constraints on Z' bosons from electroweak experiments

Following the parametrization presented in Sec. 3, we can immediately obtain the constraints on $T_{\text{new}}, \bar{\xi}$ and $g_E^2/c_\chi^2 m_{Z_2}^2$ from the data listed in Table 2 and Table 3. Setting $S_{\text{new}} = U_{\text{new}} = 0$, we find that the Z -pole measurements constrains T_{new} and $\bar{\xi}$ while m_W data constrains T_{new} . The contact term $g_E^2/c_\chi^2 m_{Z_2}^2$ is constrained from the LENC data. The number of the free parameters is, therefore, six: the above three parameters and the SM parameters, $m_t, \alpha_s(m_{Z_1})$ and $\bar{\alpha}(m_{Z_1}^2)$. Throughout our analysis, we use

$$m_t = 175.6 \pm 5.5 \text{ GeV [19]}, \quad (4.1a)$$

$$\alpha_s(m_{Z_1}) = 0.118 \pm 0.003 \text{ [13]}, \quad (4.1b)$$

$$1/\bar{\alpha}(m_{Z_1}^2) = 128.75 \pm 0.09 \text{ [21]}, \quad (4.1c)$$

as constraints on the SM parameters. The Higgs mass dependence of the results are parametrized by x_H (3.10) in the range $77 \text{ GeV} < m_H \lesssim 150 \text{ GeV}$. The lower bound is obtained at the LEP experiment [34]. The upper bound is the theoretical limit on the lightest Higgs boson mass in any supersymmetric models that accommodate perturbative unification of the gauge couplings [35]. We first obtain the constraints from the Z -pole experiments and W boson mass measurement only, and then obtain those by including the LENC experiments.

4.1 Constraints from Z -pole and m_W data

Let us examine first the constraints from the Z -pole and m_W data by performing the five-parameter fit for $T_{\text{new}}, \bar{\xi}, m_t, \alpha_s(m_{Z_1})$ and $\bar{\alpha}(m_{Z_1}^2)$. The results for the χ, ψ, η and ν models at $\delta = 0$ are summarized as follows:

(i) χ -model ($\delta = 0$)

$$\left. \begin{aligned} T_{\text{new}} &= -0.040 + 0.15x_H \pm 0.12 \\ \bar{\xi} &= 0.00017 - 0.00005x_H \pm 0.00046 \\ \chi_{\text{min}}^2/(\text{d.o.f.}) &= (16.5 + 0.7x_H)/(12), \end{aligned} \right\} \rho_{\text{corr}} = 0.28, \quad (4.2)$$

(ii) ψ -model ($\delta = 0$)

$$\left. \begin{aligned} T_{\text{new}} &= -0.043 + 0.16x_H \pm 0.11 \\ \bar{\xi} &= 0.00019 + 0.00012x_H \pm 0.00050 \\ \chi_{\text{min}}^2/(\text{d.o.f.}) &= (16.5 + 0.4x_H)/(12), \end{aligned} \right\} \rho_{\text{corr}} = 0.20, \quad (4.3)$$

(iii) η -model ($\delta = 0$)

$$\left. \begin{aligned} T_{\text{new}} &= -0.053 + 0.14x_H \pm 0.11 \\ \bar{\xi} &= -0.00014 - 0.00062x_H \pm 0.00108 \\ \chi_{\text{min}}^2/(\text{d.o.f.}) &= (16.6 + 0.4x_H)/(12), \end{aligned} \right\} \rho_{\text{corr}} = 0.09, \quad (4.4)$$

(iv) ν -model ($\delta = 0$)

$$\left. \begin{aligned} T_{\text{new}} &= -0.042 + 0.15x_H \pm 0.11 \\ \bar{\xi} &= 0.00016 + 0.00007x_H \pm 0.00042 \\ \chi_{\text{min}}^2/(\text{d.o.f.}) &= (16.5 + 0.5x_H)/(12). \end{aligned} \right\} \rho_{\text{corr}} = 0.23, \quad (4.5)$$

In the above four Z' models, the results for T_{new} and $\bar{\xi}$ are consistent with zero for $x_H = 0$. Moreover, the best fits of T_{new} in all the Z' models are in the unphysical region, $T_{\text{new}} < 0$. The parameter T_{new} could be positive for the large x_H : For example, $x_H = 0.41$ ($m_H = 150$ GeV) makes T_{new} in all the four Z' models positive. The allowed range of the effective mixing angle $\bar{\xi}$ is order of 10^{-3} for the η -model and 10^{-4} for the other three models in $1\text{-}\sigma$ level. The x_H -dependence of $\bar{\xi}$ in the η -model is larger than the other three models. For comparison, we show the result for the leptophobic η -model ($\delta = 1/3$)

(v) leptophobic η -model ($\delta = 1/3$)

$$\left. \begin{aligned} T_{\text{new}} &= -0.049 + 0.15x_H \pm 0.11 \\ \bar{\xi} &= 0.00269 + 0.00026x_H \pm 0.00309 \\ \chi_{\text{min}}^2/(\text{d.o.f.}) &= (15.9 + 0.5x_H)/(12). \end{aligned} \right\} \rho_{\text{corr}} = 0.03, \quad (4.6)$$

By comparing the η -model with no kinetic mixing ($\delta = 0$) in eq. (4.4), we find significantly weaker constraint on $\bar{\xi}$. In Fig. 1, we show the $1\text{-}\sigma$ and 90% CL allowed region on the $(\bar{\xi}, T_{\text{new}})$ plane in the η -model with $\delta = 0$ and $1/3$ for $m_H = 100$ GeV.

The best fit results at $m_H = 100$ GeV under the constraint $T_{\text{new}} \geq 0$ are shown in Table 2. We can see from Table 2 that there is no noticeable improvement of the fit for the χ, ψ, η and ν models at $\delta = 0$. The χ_{min}^2 remains almost the same as that of the SM, even though each model has two new free parameters, T_{new} and

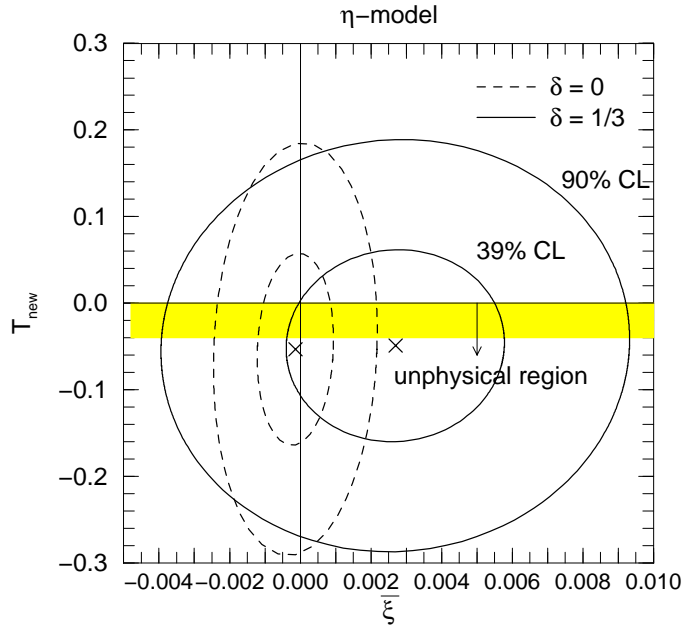


Figure 1: The $1\text{-}\sigma$ and 90% CL allowed region on the $(\bar{\xi}, T_{\text{new}})$ plane in the η -model with $\delta = 0$ and $1/3$. The shaded region ($T_{\text{new}} < 0$) corresponds to the unphysical region.

$\bar{\xi}$. The fit slightly improves for the leptophobic η -model ($\delta = 1/3$) because of the smaller pull factor for the R_b data. The probability of the fit, 18.7% CL, is still less than that of the SM, 26.2% CL, because the χ^2_{min} reduces only 0.8 despite two additional free parameters.

We explore the whole range of the parameters, β_E and δ . In Fig. 2, we show the improvement in χ^2_{min} over the SM value, $\chi^2_{\text{min}}(\text{SM}) = 16.9$ (see Table 2):

$$\Delta\chi^2 \equiv \chi^2_{\text{min}}(\beta_E, \delta) - \chi^2_{\text{min}}(\text{SM}), \quad (4.7)$$

where $\chi^2_{\text{min}}(\beta_E, \delta)$ is evaluated at the specific value of β_E and δ for $m_H = 100$ GeV. As we seen from Fig. 2, the χ^2_{min} depends very mildly in the whole range of the β_E and δ plane, except near the leptophobic η -model ($\beta_E = \tan^{-1}(\sqrt{5}/3)$ and $\delta = 1/3$) [10]. Even for the best choice of β_E and δ , the improvement in χ^2_{min} is only 1.5 over the SM. Because each model has two additional parameters T_{new} and $\bar{\xi}$, we can conclude that no Z' model in this framework improves the fit over the SM. The “ \times ” marks plotted in Fig. 2 show the specific models which we will discuss in the next section.

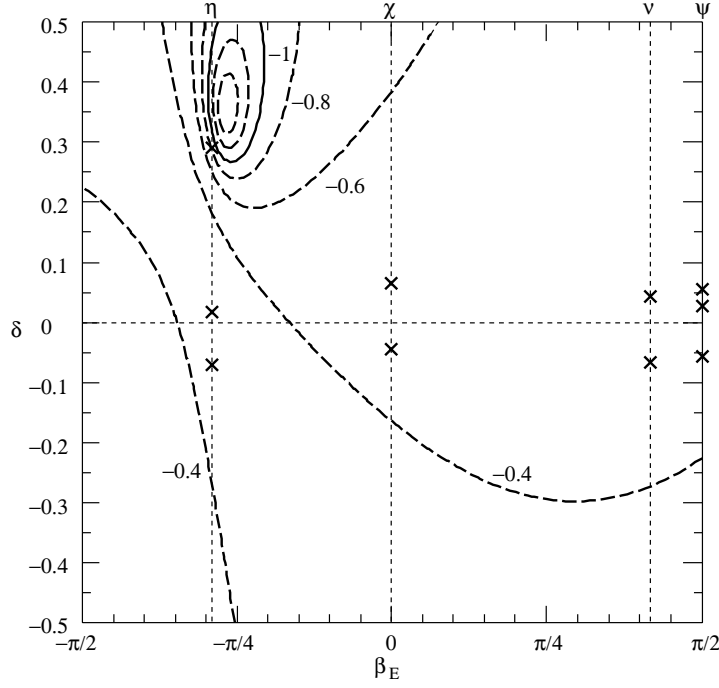


Figure 2: Contour plot of $\Delta\chi^2 \equiv \chi_{\min}^2(\beta, \delta) - \chi_{\min}^2(\text{SM})$ for $m_H = 100$ GeV. The mixing angle β_E for the χ, ψ, η and ν models are shown by vertical dotted lines. The step of each contour is 0.2. The “ \times ” marks on the plot show the specific models listed in Table 8 in Sec. 5.

4.2 Constraints from Z -pole + m_W + LENC data

Next we find constraints on the contact term $g_E^2/c_\chi^2 m_{Z_2}^2$ by including the low-energy data in addition to the Z -pole and m_W data. Because T_{new} and $\bar{\xi}$ are already constrained severely by the Z -pole and m_W data, only the contact terms proportional to $g_E^2/c_\chi^2 m_{Z_2}^2$ contribute to the low-energy observables, except for the special case of the leptophobic η -model ($\delta = 1/3$).

We summarize the results of the six-parameter fit for the ψ, χ, η and ν models:

(i) χ -model

$$\left. \begin{aligned} T_{\text{new}} &= -0.063 + 0.14x_H \pm 0.11 \\ \bar{\xi} &= -0.00005 - 0.00006x_H \pm 0.00044 \\ g_E^2/c_\chi^2 m_{Z_2}^2 &= 0.26 + 0.01x_H \pm 0.21 \end{aligned} \right\} \rho_{\text{corr}} = \begin{pmatrix} 1.00 & 0.25 & 0.09 \\ & 1.00 & 0.15 \\ & & 1.00 \end{pmatrix}, \quad (4.8a)$$

$$\chi_{\min}^2/(\text{d.o.f.}) = (19.9 + 0.9x_H)/(20), \quad (4.8b)$$

(ii) ψ -model

$$\left. \begin{aligned} T_{\text{new}} &= -0.065 + 0.15x_H \pm 0.11 \\ \bar{\xi} &= -0.00014 + 0.00012x_H \pm 0.00050 \\ g_E^2/c_\chi^2 m_{Z_2}^2 &= 1.66 + 0.19x_H \pm 2.90 \end{aligned} \right\} \rho_{\text{corr}} = \begin{pmatrix} 1.00 & 0.19 & 0.07 \\ & 1.00 & 0.03 \\ & & 1.00 \end{pmatrix}, \quad (4.9a)$$

$$\chi_{\min}^2/(\text{d.o.f.}) = (21.1 + 0.8x_H)/(20), \quad (4.9b)$$

(iii) η -model

$$\left. \begin{aligned} T_{\text{new}} &= -0.074 + 0.14x_H \pm 0.11 \\ \bar{\xi} &= -0.00038 - 0.00063x_H \pm 0.00106 \\ g_E^2/c_\chi^2 m_{Z_2}^2 &= -0.62 + 0.08x_H \pm 0.87 \end{aligned} \right\} \rho_{\text{corr}} = \begin{pmatrix} 1.00 & 0.06 & -0.05 \\ & 1.00 & -0.22 \\ & & 1.00 \end{pmatrix}, \quad (4.10a)$$

$$\chi_{\min}^2/(\text{d.o.f.}) = (20.8 + 0.5x_H)/(20), \quad (4.10b)$$

(iv) ν -model

$$\left. \begin{aligned} T_{\text{new}} &= -0.061 + 0.15x_H \pm 0.11 \\ \bar{\xi} &= 0.00010 + 0.00006x_H \pm 0.00041 \\ g_E^2/c_\chi^2 m_{Z_2}^2 &= -0.65 + 0.04x_H \pm 0.54 \end{aligned} \right\} \rho_{\text{corr}} = \begin{pmatrix} 1.00 & 0.21 & 0.07 \\ & 1.00 & 0.03 \\ & & 1.00 \end{pmatrix}, \quad (4.11a)$$

$$\chi_{\min}^2/(\text{d.o.f.}) = (20.1 + 0.8x_H)/(20). \quad (4.11b)$$

The contact term $g_E^2/c_\chi^2 m_{Z_2}^2$ in the ψ and η models is consistent with zero in 1- σ level. Both the best fit and the 1- σ error of the parameters T_{new} and $\bar{\xi}$ in all the Z' models are slightly affected by including the LENC data: The best fit value of T_{new} in all the Z' models cannot be positive even for the $m_H = 150$ GeV ($x_H = 0.41$). Since the leptophobic η -model does not have the contact term, the low-energy data constrain the same parameters T_{new} and $\bar{\xi}$. After taking into account both the high-energy and low-energy data, we find

(v) leptophobic η model ($\delta = 1/3$)

$$\left. \begin{aligned} T_{\text{new}} &= -0.074 + 0.148x_H \pm 0.110 \\ \bar{\xi} &= 0.00157 + 0.00019x_H \pm 0.00279 \\ \chi_{\min}^2/(\text{d.o.f.}) &= (21.2 + 1.0x_H)/(21). \end{aligned} \right\} \rho_{\text{corr}} = 0.02, \quad (4.12)$$

The allowed range of $\bar{\xi}$ is slightly severe as compared to eq. (4.6).

The best fit results for $m_H = 100$ GeV under the condition $T_{\text{new}} \geq 0$ are shown in Table 3. It is noticed that the best fit values for the weak charge of cesium atom ^{133}Cs in the χ, η and ν models are quite close to the experimental data. These models lead to $\Delta\chi^2 = -1.8$ (χ), -0.8 (η) and -1.6 (ν). No other noticeable point is found in the table.

The above constraints on $g_E^2/c_\chi^2 m_{Z_2}^2$ from the LENC data give the lower mass bound of the heavier mass eigenstate Z_2 in the Z' models except for the leptophobic η -model. In Fig. 3, the contour plot of the 95% CL lower mass limit of Z_2 boson from the LENC experiments are shown on the (β_E, δ) plane by setting $g_E = g_Y$

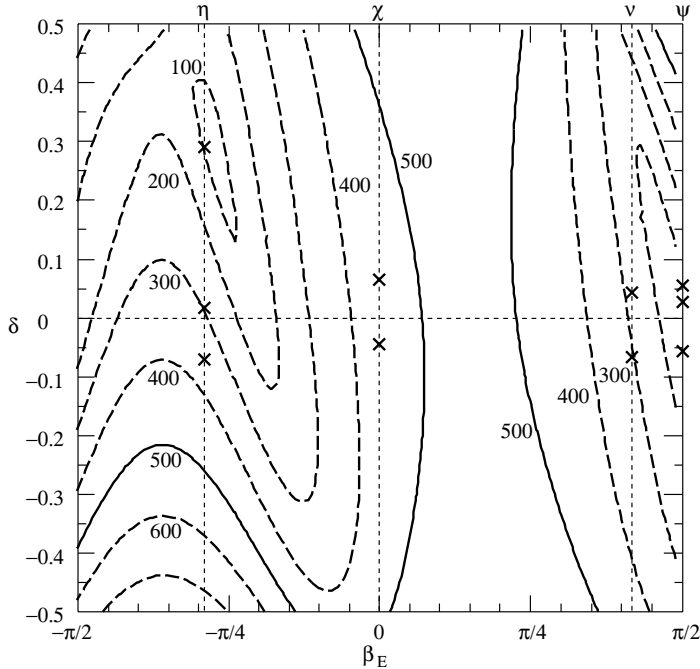


Figure 3: Contour plot of the 95% CL lower mass limit of the Z_2 boson obtained from the LENC experiments for $g_E = g_Y$ and $m_H = 100$ GeV. The vertical dotted lines correspond to the χ, ψ, η and ν models. The limits are given in the unit of GeV. The “x” marks on the plot show the specific models listed in Table 8 in Sec. 5.

and $m_H = 100$ GeV under the condition $m_{Z_2} \geq 0$. In practice, we obtain the 95% CL lower limit of the Z_2 boson mass m_{95} in the following way:

$$0.05 = \frac{\int_{m_{95}}^{\infty} dm_{Z_2} P(m_{Z_2})}{\int_0^{\infty} dm_{Z_2} P(m_{Z_2})}, \quad (4.13)$$

where we assume that the probability density function $P(m_{Z_2})$ is proportional to $\exp(-\chi^2(m_{Z_2})/2)$.

We can read off from Fig. 3 that the lower mass bound of the Z_2 boson in the ψ model at $\delta = 0$ is much weaker than those of the other Z' models. It has been pointed out that the most stringent constraint on the contact term is the APV measurement of cesium atom [6]. Since all the SM matter fields in the ψ model have the same $U(1)'$ charge (see Table 1), the couplings of contact interactions are Parity conserving, which makes constraint from the APV measurement useless. We also find in Fig. 3 that the lower mass bound of the Z_2 boson disappears near the leptophobic η -model ($\beta_E = \tan^{-1}(\sqrt{5/3})$ and $\delta = 1/3$) [10].

We summarize the 95% CL lower bound on m_{Z_2} for the χ, ψ, η and ν models ($\delta = 0$) in Table 5. For comparison, we also show the lower bound of m_{Z_2} in the

Table 5: The 95% CL lower bound of m_{Z_2} (GeV) in the χ, ψ, η and ν models ($\delta = 0$) for $g_E = g_Y$ and $m_H = 100$ GeV. The results of previous study [36] and of recent direct search [37] are shown for comparison.

	χ	ψ	η	ν
Our results	451	136	317	284
Langacker <i>et al.</i> [36]	330	170	220	—
direct search [37]	595	590	620	—

previous study [36] in the same table. The bounds on the Z_χ and Z_ν masses are more severely constrained as compared to ref. [36]. Although we used the latest electroweak data, our result for the Z_ψ boson mass is somewhat weaker than that of ref. [36]. In the analysis of ref. [36], the $e^+e^- \rightarrow \mu^+\mu^-, \tau^+\tau^-$ data below the Z pole are also used besides the Z -pole, m_W and the LENC data. As we mentioned before, the lower mass bound of the Z' boson is obtained from the LENC data, not from the Z -pole data. Because the APV measurement which is most stringent constraint in the LENC data does not well constrain the ψ model, it is expected that the e^+e^- annihilation data below the Z -pole play an important role to obtain the bound of Z_ψ boson mass.

Our results in Table 5 are also slightly weaker than those in ref. [6]. The results in ref. [6] have been obtained without including the Z - Z' mixing effects and by setting $m_t = 175$ GeV, $m_H = 100$ GeV, $x_\alpha = 0$ and $T_{\text{new}} = 0$.

4.3 Lower mass bound of Z_2 boson

We have found that the Z -pole, m_W and the LENC data constrain $(T_{\text{new}}, \bar{\xi})$, T_{new} and $g_E^2/c_\chi^2 m_{Z_2}^2$, respectively. We can see from eq. (2.17) that, for a given ζ , constraints on $T_{\text{new}}, \bar{\xi}$ and $g_E^2/c_\chi^2 m_{Z_2}^2$ can be interpreted as the bound on m_{Z_2} . We show the 95% CL lower mass bound of the Z_2 boson for $m_H = 100$ GeV in four Z' models as a function of ζ . The bound is again found under the condition $m_{Z_2} \geq 0$. Results are shown in Fig. 4.(a) \sim 4.(d) for the χ, ψ, η, ν models, respectively. The lower bound from the Z -pole and m_W data, and that from the LENC data are separately plotted in the same figure. In order to see the g_E -dependence of the m_{Z_2} bound explicitly, we show the lower mass bound for the combination $m_{Z_2} g_Y / g_E$. We can read off from Fig. 4 that the bound on $m_{Z_2} g_Y / g_E$ is approximately independent of g_E for $g_E / g_Y = 0.5 \sim 2.0$ in each model. As we expected from the formulae for T_{new} and $\bar{\xi}$ in the small mixing limit (eq. (2.16)), the Z_2 mass

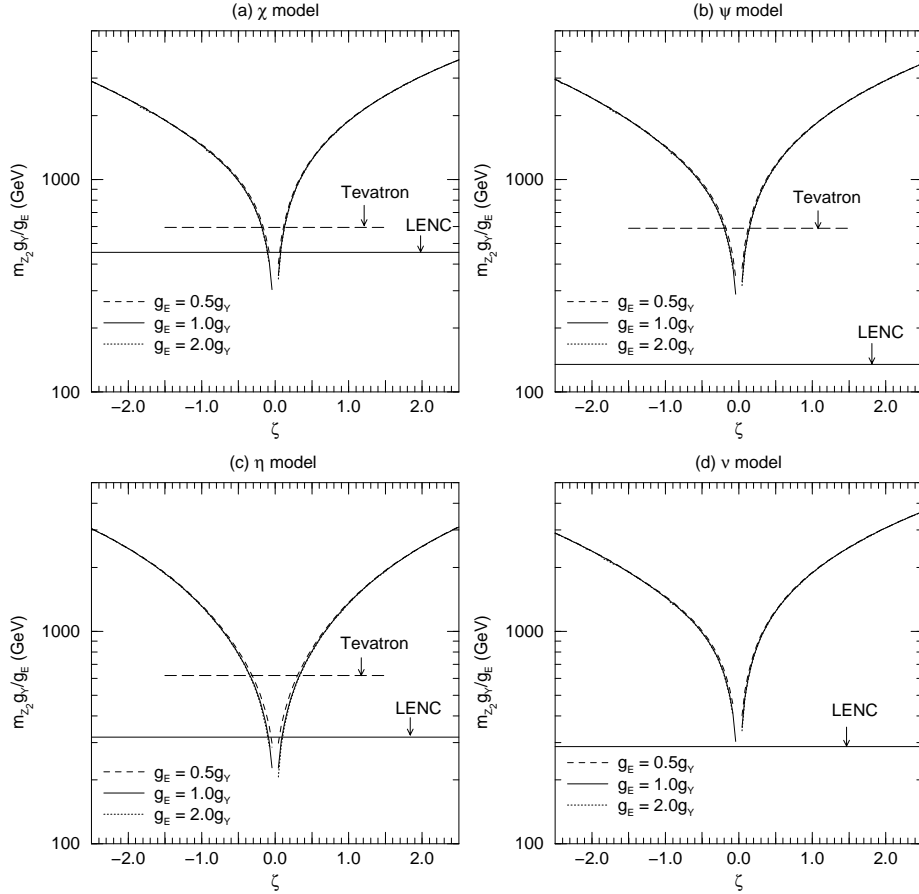


Figure 4: The 95% CL lower mass limit of Z_2 in the χ , ψ , η and ν models for $m_H = 100$ GeV. The Z_2 boson mass is normalized by g_E/g_Y . Constraints from Z -pole experiments and LENC experiments are separately shown. The results of the direct search at Tevatron [37] for the χ , ψ and η models are also shown.

is unbounded from the Z -pole data at $\zeta = 0$. For models with very small ζ , the lower bound on m_{Z_2} , therefore, comes from the LENC experiments and the direct search experiment at Tevatron. For comparison, we plot the 95% CL lower bound on m_{Z_2} obtained from the direct search experiment [37] in Fig. 4. In the direct search experiment, the Z' decays into the exotic particles, *e.g.*, the decays into the light right-handed neutrinos which are expected for some models, are not taken into account. We summarize the 95% CL lower bound on m_{Z_2} for the χ , ψ , η and ν models ($\delta = 0$) obtained from the low-energy data and the direct search experiment [37] in Table 5.

The lower bound of m_{Z_2} is affected by the Higgs boson mass through the T parameter. As we seen from eqs. (4.2) \sim (4.5), T_{new} tends to be in the physical

region ($T_{\text{new}} \geq 0$) for large m_H (x_H). Then, we find that the large Higgs boson mass decreases the lower bound of m_{Z_2} . For $\zeta = 1$, the lower m_{Z_2} bound in the χ, ψ, ν (η) models for $m_H = 150$ GeV is weaker than that for $m_H = 100$ GeV about 7% (11%). On the other hand, the Higgs boson with $m_H = 80$ GeV makes the lower m_{Z_2} bound in all the Z' models severe about 5% as compared to the case for $m_H = 100$ GeV. Because T_{new} and $\bar{\xi}$ are proportional to ζ^2 and ζ , respectively (see eq. (2.16)), and it is unbounded at $|\zeta| \simeq 0$, the lower bound of m_{Z_2} may be independent of m_H in the small $|\zeta|$ region. The m_H -dependence of the lower mass bound obtained from the LENC data is safely negligible.

It should be noted that, at $\zeta = 0$, only the leptophobic η -model ($\delta = 1/3$) is not constrained from both the Z -pole and the low-energy data. The precise analysis and discussion for the lower mass bound of the Z_2 boson in the leptophobic η -model can be found in ref. [38]. It is shown in ref. [38] that the ζ -dependence of the lower mass bound is slightly milder than that of the η -model with $\delta = 0$ in Fig. 4.(c).

It has been discussed that the presence of Z_2 boson whose mass is much heavier than the SM Z boson mass, say 1 TeV, may lead to a fine-tuning problem to stabilize the electroweak scale against the $U(1)'$ scale [39]. The Z_2 boson with $m_{Z_2} \leq 1$ TeV for $g_E = g_Y$ is allowed by the electroweak data only if ζ satisfies the following condition:

$$\begin{aligned} -0.6 \lesssim \zeta \lesssim +0.3 & \quad \text{for the } \chi, \psi, \nu \text{ models,} \\ -0.7 \lesssim \zeta \lesssim +0.6 & \quad \text{for the } \eta \text{ model.} \end{aligned} \tag{4.14}$$

In principle, the parameter ζ is calculable, together with the gauge coupling g_E , once the particle spectrum of the E_6 model is specified. In the next section, we calculate the ζ parameter in several E_6 Z' models.

5 Light Z' boson in minimal SUSY E_6 -models

It is known that the gauge couplings are not unified in the E_6 models with three generations of **27**. In order to guarantee the gauge coupling unification, a pair of weak-doublets, H' and \overline{H}' , should be added into the particle spectrum at the electroweak scale [40]. They could be taken from **27** + $\overline{\mathbf{27}}$ or the adjoint representation **78**. The $U(1)'$ charges of the additional weak doublets should have the same magnitude and opposite sign, a and $-a$, to cancel the $U(1)'$ anomaly. In addition, a pair of the complete $SU(5)$ multiplet such as **5** + $\overline{\mathbf{5}}$ can be added without spoiling the unification of the gauge couplings [10, 40].

Table 6: Charge assignment for the extra weak doublets in the minimal E_6 model and the η_{BKM} model of ref. [10]. The symbol $a_i(-a_i)$ for $i = \chi, \psi, \eta, \nu$ are the $U(1)'$ charge of L or H_d (H_u).

	field	Y	$2\sqrt{6}Q_\chi$	$\sqrt{72/5}Q_\psi$	Q_η	Q_ν
minimal model	H'	$-\frac{1}{2}$	a_χ	a_ψ	a_η	a_ν
	\overline{H}'	$+\frac{1}{2}$	$-a_\chi$	$-a_\psi$	$-a_\eta$	$-a_\nu$
η_{BKM} model [10]	H'_1	$-\frac{1}{2}$			1	
	\overline{H}_1	$+\frac{1}{2}$			-1	
	H'_2	$-\frac{1}{2}$			1	
	\overline{H}_2	$+\frac{1}{2}$			-1	
	D'	$-\frac{1}{3}$			$\frac{2}{3}$	
	\overline{D}'	$+\frac{1}{3}$			$-\frac{2}{3}$	

The minimal E_6 model which have three generations of $\mathbf{27}$ and a pair $\mathbf{2} + \overline{\mathbf{2}}$ depends in principle on the three cases; H' has the same quantum number as L or H_d of $\mathbf{27}$, or \overline{H}_u of $\overline{\mathbf{27}}$. All three cases will be studied below. The hypercharge and $U(1)'$ charge of the extra weak doublets for the χ, ψ, η, ν models are listed in Table 6. For comparison, we also show those in the model of Babu *et al.* [10], where two pairs of $\mathbf{2} + \overline{\mathbf{2}}$ from $\mathbf{78}$ and a pair of $\mathbf{3} + \overline{\mathbf{3}}$ from $\mathbf{27} + \overline{\mathbf{27}}$ are introduced to achieve the quasi-leptophobia at the weak scale.

Let us recall the definition of ζ ;

$$\zeta = \frac{g_Z}{g_E} \frac{m_{ZZ'}^2}{m_Z^2} - \delta. \quad (5.1)$$

In the minimal model, the following eight scalar-doublets can develop VEV to give the mass terms m_Z^2 and $m_{ZZ'}^2$ in eq. (2.4): three generations of H_u, H_d , and an extra pair, H' and \overline{H}' . Then, m_Z^2 and $m_{ZZ'}^2$ are written in terms of their VEVs as

$$m_Z^2 = \frac{1}{2} g_Z^2 \left[\sum_{i=1}^3 \left\{ \langle H_u^i \rangle^2 + \langle H_d^i \rangle^2 \right\} + \langle H' \rangle^2 + \langle \overline{H}' \rangle^2 \right], \quad (5.2a)$$

$$m_{ZZ'}^2 = g_Z g_E \left[\sum_{i=1}^3 \left\{ -Q_E^{H_u} \langle H_u^i \rangle^2 + Q_E^{H_d} \langle H_d^i \rangle^2 \right\} + Q_E^{H'} \langle H' \rangle^2 - Q_E^{\overline{H}'} \langle \overline{H}' \rangle^2 \right], \quad (5.2b)$$

where i is the generation index. The third component of the weak isospin I_3 for

the Higgs fields are

$$I_3(H_d) = I_3(H') = -I_3(H_u) = -I_3(\overline{H'}) = 1/2. \quad (5.3)$$

Taking account of the U(1)' charges of the extra Higgs doublets, $Q_E^{H'} = -Q_E^{\overline{H'}}$, we find from eq. (5.1)

$$\zeta = 2 \frac{\sum_{i=1}^3 \left\{ -Q_E^{H_u} \langle H_u^i \rangle^2 + Q_E^{H_d} \langle H_d^i \rangle^2 \right\} + Q_E^{H'} \left(\langle H' \rangle^2 + \langle \overline{H'} \rangle^2 \right)}{\sum_{i=1}^3 \left\{ \langle H_u^i \rangle^2 + \langle H_d^i \rangle^2 \right\} + \langle H' \rangle^2 + \langle \overline{H'} \rangle^2} - \delta. \quad (5.4)$$

We note here that the observed μ -decay constant leads to the following sum rule

$$v_u^2 + v_d^2 + v_{H'}^2 + v_{\overline{H'}}^2 \equiv v^2 = \frac{1}{\sqrt{2}G_F} \approx (246 \text{ GeV})^2, \quad (5.5)$$

where

$$\begin{aligned} \sum_{i=1}^3 \langle H_u^i \rangle^2 &= \frac{v_u^2}{2}, & \sum_{i=1}^3 \langle H_d^i \rangle^2 &= \frac{v_d^2}{2}, \\ \langle H' \rangle^2 &= \frac{v_{H'}^2}{2}, & \langle \overline{H'} \rangle^2 &= \frac{v_{\overline{H'}}^2}{2}. \end{aligned} \quad (5.6)$$

By further introducing the notation

$$\tan \beta = \frac{v_u}{v_d}, \quad (5.7a)$$

$$x^2 = \frac{v_{H'}^2 + v_{\overline{H'}}^2}{v^2}, \quad (5.7b)$$

we can express eq. (5.4) as

$$\zeta = 2 \left\{ -Q_E^{H_u} (1 - x^2) \sin^2 \beta + Q_E^{H_d} (1 - x^2) \cos^2 \beta + Q_E^{H'} x^2 \right\} - \delta. \quad (5.8)$$

Because H' and $\overline{H'}$ are taken from $\mathbf{27} + \overline{\mathbf{27}}$, the U(1)' charge of H' , $Q_E^{H'}$, is identified with that of L , H_d or $\overline{H_u}$.

Among all the models, only in the χ -model one can have smaller number of matter particles. In the χ -model, three generations of the matter fields $\mathbf{16}$ and a pair of Higgs doublets make the model anomaly free. In this case, ζ is found to be independent of $\tan \beta$:

$$\zeta = 2 \frac{Q_E^{H_d} - Q_E^{H_u} \tan^2 \beta}{1 + \tan^2 \beta} - \delta \quad (5.9a)$$

$$= 2Q_E^{H_d} - \delta. \quad (5.9b)$$

Table 7: Coefficients of the 1-loop β -functions for the gauge couplings in the MSSM, the minimal E_6 models and the η_{BKM} model [10]. The model $\chi(16)$ has three generations of $\mathbf{16}$ and a pair $\mathbf{2} + \bar{\mathbf{2}}$. The model $\chi(27)$ and ψ, η, ν have three generations of $\mathbf{27}$ and a pair $\mathbf{2} + \bar{\mathbf{2}}$.

	MSSM	$\chi(16)$	$\chi(27)$	ψ	η	ν	η_{BKM} [10]
b_1	$\frac{33}{5}$	$\frac{33}{5}$	$\frac{48}{5}$	$\frac{48}{5}$	$\frac{48}{5}$	$\frac{48}{5}$	$\frac{53}{5}$
b_2	1	1	4	4	4	4	5
b_3	-3	-3	0	0	0	0	1
b_E	—	$6 + \frac{a^2}{10}$	$9 + \frac{a^2}{10}$	$9 + \frac{a^2}{6}$	$9 + \frac{12}{5}a^2$	$9 + \frac{12}{5}a^2$	$\frac{77}{5}$
b_{1E}	—	$-\sqrt{\frac{3}{50}}a$	$-\sqrt{\frac{3}{50}}a$	$-\sqrt{\frac{1}{10}}a$	$-\frac{6}{5}a$	$-\frac{6}{5}a$	$-\frac{16}{5}$

Let us now examine the kinetic mixing parameter δ in each model. The boundary condition of δ at the GUT scale is $\delta = 0$. The non-zero kinetic mixing term can arise at low-energy scale through the following RGEs:

$$\frac{d}{dt}\alpha_i = \frac{1}{2\pi}b_i\alpha_i^2, \quad (5.10a)$$

$$\frac{d}{dt}\alpha_4 = \frac{1}{2\pi}(b_E + 2b_{1E}\delta + b_1\delta^2)\alpha_4^2, \quad (5.10b)$$

$$\frac{d}{dt}\delta = \frac{1}{2\pi}(b_{1E} + b_1\delta)\alpha_1, \quad (5.10c)$$

where $i = 1, 2, 3$ and $t = \ln \mu$. We define α_1 and α_4 as

$$\alpha_1 \equiv \frac{5}{3} \frac{g_Y^2}{4\pi}, \quad \alpha_4 \equiv \frac{5}{3} \frac{g_E^2}{4\pi}. \quad (5.11)$$

The coefficients of the β -functions for α_1, α_4 and δ are:

$$b_1 = \frac{3}{5}\text{Tr}(Y^2), \quad b_E = \frac{3}{5}\text{Tr}(Q_E^2), \quad b_{1E} = \frac{3}{5}\text{Tr}(YQ_E). \quad (5.12)$$

From eq. (5.10c), we can clearly see that the non-zero δ is generated at the weak scale if $b_{1E} \neq 0$ holds. In Table 7, we list b_1, b_E and b_{1E} in the minimal χ, ψ, η, ν models and the η_{BKM} model [10]. As explained above, the $\chi(16)$ model has three generations of $\mathbf{16}$, and the $\chi(27)$ model has three generations of $\mathbf{27}$. We can see

Table 8: Predictions for g_E and δ at $\mu = m_{Z_1}$ in the minimal models and the η_{BKM} model [10]. The $U(1)_Y$ gauge coupling g_Y is fixed as $g_Y = 0.36$.

model	a	g_E	g_E/g_Y	δ
$\chi(16)$	3	0.353	0.989	0.066
	-2	0.361	1.010	-0.044
$\chi(27)$	3	0.353	0.989	0.066
	-2	0.361	1.010	-0.044
ψ	1	0.364	1.020	0.028
	2	0.356	0.999	0.056
	-2	0.356	0.999	-0.056
η	1/6	0.366	1.025	0.018
	-2/3	0.351	0.982	-0.071
ν	$\sqrt{1/6}$	0.361	1.010	0.044
	$-\sqrt{3/8}$	0.353	0.989	-0.066
η_{BKM} [10]	—	0.308	0.862	0.286

from Table 7 that the magnitudes of the differences $b_1 - b_2$ and $b_2 - b_3$ are common among all the models including the minimal supersymmetric SM. This guarantees the gauge coupling unification at $\mu = m_{GUT} \simeq 10^{16}$ GeV.

It is straightforward to obtain $g_E(m_{Z_1})$ and $\delta(m_{Z_1})$ for each model. The analytical solutions of eqs. (5.10a)~(5.10c) are as follows:

$$\frac{1}{\alpha_i(m_{Z_1})} = \frac{1}{\alpha_{GUT}} + \frac{1}{2\pi} b_i \ln \frac{m_{GUT}}{m_{Z_1}}, \quad (5.13a)$$

$$\delta(m_{Z_1}) = -\frac{b_{1E}}{b_1} \left(1 - \frac{\alpha_1(m_{Z_1})}{\alpha_{GUT}} \right), \quad (5.13b)$$

$$\frac{1}{\alpha_4(m_{Z_1})} = \frac{1}{\alpha_{GUT}} + \left\{ \frac{b_E}{b_1} - \left(\frac{b_{1E}}{b_1} \right)^2 \right\} \left\{ \frac{1}{\alpha_1(m_{Z_1})} - \frac{1}{\alpha_{GUT}} \right\} - \left(\frac{b_{1E}}{b_1} \right)^2 \frac{\alpha_1(m_{Z_1}) - \alpha_{GUT}}{\alpha_{GUT}^2}, \quad (5.13c)$$

where α_{GUT} denotes the unified gauge coupling at $\mu = m_{GUT}$. In our calculation, $\alpha_3(m_{Z_1}) = 0.118$ and $\alpha(m_{Z_1}) = e^2(m_{Z_1})/4\pi = 1/128$ are used as example. These numbers give $g_Y(m_{Z_1}) = 0.357$. We summarize the predictions for g_E and δ at $\mu = m_{Z_1}$ in the minimal E_6 models and the η_{BKM} model in Table 8. In all the

Table 9: Predictions for the effective Z - Z' mixing parameter ζ in the minimal χ, ψ, η, ν and the η_{BKM} model for $x^2 = 0$ and 0.5 , and $\tan \beta = 2$ and 30 .

		$x^2 = 0$		$x^2 = 0.5$	
		$\tan \beta$		$\tan \beta$	
	a	2	30	2	30
χ	3	-0.88		0.14	
	-2	-0.77			
ψ	1	0.60	1.02	0.55	0.76
	2	0.58	1.00	0.79	1.00
	-2	0.69	1.11	-0.16	0.06
η	1/6	-1.02	-1.35	-0.35	-0.52
	-2/3	-0.93	-1.26	-1.11	-1.26
ν	$\sqrt{1/6}$	0.36	0.77	0.57	0.77
	$-\sqrt{3/8}$	0.47	0.88	-0.34	-0.14
η_{BKM}	—	-1.29	-1.62	-1.79	-1.95

minimal models, the ratio g_E/g_Y is approximately unity and $|\delta|$ is smaller than about 0.07. On the other hand, the η_{BKM} model predicts $g_E/g_Y \sim 0.86$ and $\delta \sim 0.29$, which is close to the leptophobic- η model at $\delta = 1/3$. In Figs. 2 and 3, we show the predictions of all the models by “ \times ” symbol.

Next, we estimate the parameter ζ for several sets of $\tan \beta$ and x . In Table 9, we show the predictions for ζ in the minimal χ, ψ, η, ν models and the η_{BKM} model. The results are shown for $\tan \beta = 2$ and 30 , and $x^2 = 0$ and 0.5 . We find from the table that the parameter ζ is in the range $|\zeta| \lesssim 1.35$ for all the models except for the η_{BKM} model, where the predicted ζ lies between -2.0 and -1.2 . It is shown in Fig. 4 that $m_{Z_2} g_Y/g_E$ is approximately independent of g_E/g_Y . Actually, we find in Table 8 and Table 9 that the predicted $|\delta|$ is smaller than about 0.1 and g_E/g_Y is quite close to unity in all the minimal models. We can, therefore, read off from Fig. 4 the lower bound of m_{Z_2} in the minimal models at $g_E = g_Y$. In Table 10, we summarize the 95% CL lower m_{Z_2} bound for the minimal χ, ψ, η, ν models and the η_{BKM} model which correspond to the predicted ζ in Table 9. Most of the lower mass bounds in Table 10 exceed 1 TeV. The Z_2 boson with $m_{Z_2} \sim O(1 \text{ TeV})$ should be explored at the future collider such as LHC. The discovery limit of the Z' boson in the E_6 models at LHC is expected as [41]

χ	ψ	η	ν
3040	2910	2980	***

(5.14)

Table 10: Summary of the 95% CL lower bound of m_{Z_2} (GeV) which corresponds to the predicted ζ in Table 9.

		$x^2 = 0$		$x^2 = 0.5$	
		$\tan \beta$		$\tan \beta$	
	a	2	30	2	30
χ	3	1330		620	
	-2	1230			
ψ	1	1290	1800	1220	1480
	2	1250	1750	1510	1750
	-2	1380	1890	520	370
η	+1/6	1330	1690	620	790
	-2/3	1230	1590	1410	1590
ν	$-\sqrt{3/8}$	1180	1720	800	520
	$+\sqrt{1/6}$	1030	1580	1320	1580
η_{BKM}	—	1520	1930	2150	2360

All the lower bounds of m_{Z_2} listed in Table 10 are smaller than 2 TeV and they are, therefore, in the detectable range of LHC. But, it should be noticed that most of them ($1 \text{ TeV} \lesssim m_{Z_2}$) may require the fine-tuning to stabilize the electroweak scale against the $U(1)'$ scale [39].

The lower bound of the Z_2 boson mass in the η_{BKM} model for the predicted ζ can be read off from Fig. 2 in ref. [38]. Because somewhat large ζ is predicted in the η_{BKM} model, $1 \lesssim |\zeta|$, the lower mass bound is also large as compared to the minimal models.

6 Summary

We have studied constraints on Z' bosons in the SUSY E_6 models. Four Z' models — the χ, ψ, η and ν models are studied in detail. The presence of the Z' boson affects the electroweak processes through the effective Z - Z' mass mixing angle $\bar{\xi}$, a tree level contribution T_{new} which is a positive definite quantity, and the contact term $g_E^2/c_\chi^2 m_{Z_2}^2$. The Z -pole, m_W and LENC data constrain $(T_{\text{new}}, \bar{\xi})$, T_{new} and $g_E^2/c_\chi^2 m_{Z_2}^2$, respectively. The convenient parametrization of the electroweak observables in the SM and the Z' models are presented. From the updated electroweak data, we find that the Z' models never give the significant improvement of the χ^2 -fit even if the kinetic mixing is taken into account. The 95% CL lower

mass bound of the heavier mass eigenstate Z_2 is given as a function of the effective Z - Z' mixing parameter ζ . The approximate scaling law is found for the g_E/g_Y -dependence of the lower limit of m_{Z_2} . By assuming the minimal particle content of the E_6 model, we have found the theoretical predictions for ζ . We have shown that the E_6 models with minimal particle content which is consistent with the gauge coupling unification predict the non-zero kinetic mixing term δ and the effective mixing parameter ζ of order one. The present electroweak experiments lead to the lower mass bound of order 1 TeV or larger for those models.

Acknowledgment

This work is supported in part by Grant-in-Aid for Scientific Research from the Ministry of Education, Science and Culture of Japan.

References

- [1] The LEP Collaborations ALEPH, DELPHI, L3, OPAL, the LEP Electroweak Working Group and the SLD Heavy Flavor Group, CERN-PPE/97-154.
- [2] J. Hewett and T. Rizzo, Phys. Rep. **183** (1989) 193.
- [3] M. Cvetič *et al.*, Phys. Rev. **D56** (1997) 2861;
P. Langacker and J. Wang, hep-ph/9804428.
- [4] G. Altarelli *et al.*, Phys. Lett. **B263** (1991) 459;
F. del Aguila, W. Hollik, J.M. Moreno and M. Quiros, Nucl. Phys. **B372** (1992) 3;
G. Altarelli *et al.*, Phys. Lett. **B318** (1993) 139.
- [5] P. Langacker and M. Luo, Phys. Rev. **D45** (1992) 278;
P. Langacker, in *Precision Tests of the Standard Electroweak Model*, (ed) P. Langacker, World Scientific, (1995) 883.
- [6] G.C. Cho, K. Hagiwara and S. Matsumoto, hep-ph/9707334, to appear in Eur. Phys. J. **C**.
- [7] T. Gherghetta, T.A. Kaeding and G.L. Kane, Phys. Rev. **D57** (1998) 3178.

- [8] L3 Collaboration, Phys. Lett. **B306** (1993) 187;
ALEPH Collaboration, Z. Phys. **C62** (1994) 539.
- [9] B. Holdom, Phys. Lett. **B166** (1986) 196.
- [10] K.S. Babu, C. Kolda and J. March-Russell, Phys. Rev. **D54** (1996) 4635.
- [11] K.S. Babu, C. Kolda and J. March-Russell, Phys. Rev. **D57** (1998) 6788.
- [12] M.E. Peskin and T. Takeuchi, Phys. Rev. Lett. **65** (1990) 964; Phys. Rev. **D46** (1992) 381.
- [13] Particle Data Group, R.M. Barnett *et al.*, Phys. Rev. **D54** (1996) 1.
- [14] J. Ellis, K. Enqvist, D.V. Nanopoulos and F. Zwirner, Mod. Phys. Lett. **A1** (1986) 57; Nucl. Phys. **B276** (1986) 14.
- [15] L.E. Ibáñez and J. Mas, Nucl. Phys. **B286** (1987) 107;
T. Matsuoka, H. Mino, D. Suematsu and S. Watanebe, Prog. Theor. Phys. **76** (1986) 915.
- [16] T. Yanagida, in *Proceedings of the Workshop on the Unified Theory and the Baryon Number in the Universe*, (ed) O. Sawada and A. Sugamoto, KEK (1979);
M. Gell-Man, P. Ramond and R. Slansky, in *Supergravity*, (ed) P.von Nienhuzen and D.Z. Freedman, North Holland (1979).
- [17] K. Hagiwara, D. Haidt, C.S. Kim and S. Matsumoto, Z. Phys. **C64** (1994) 559; **C68** (1995) 352 (E).
- [18] B. Holdom, Phys. Lett. **B259** (1991) 329.
- [19] CDF Collaboration, J. Lys, talk at ICHEP96, in Proc. of ICHEP96, (ed) Z. Ajduk and A.K. Wroblewski, World Scientific, (1997);
D0 Collaboration, S. Protopopescu, talk at ICHEP96, in the proceedings.
P. Tipton, talk at ICHEP96, in the proceedings.
- [20] K. Hagiwara, D. Haidt and S. Matsumoto, Eur. Phys. J. **C2** (1998) 95.
- [21] S. Eidelman and F. Jegerlehner, Z. Phys. **C67** (1995) 585.

- [22] J.E. Kim, P. Langacker, M. Levine and H.H. Williams, *Rev. Mod. Phys.* **53** (1981) 211.
- [23] C.Y. Prescott *et al.* , *Phys. Lett.* **B84** (1979) 524.
- [24] A. Argento *et al.* , *Phys. Lett.* **B120** (1983) 245.
- [25] P.A. Souder, in *Precision tests of the standard electroweak model*, (ed) P. Langacker, World Scientific (1995), 599.
- [26] P.A. Souder *et al.* , *Phys. Rev. Lett.* **65** (1990) 694.
- [27] W. Heil *et al.* , *Nucl. Phys.* **B327** (1989) 1.
- [28] W.J. Marciano and A. Sirlin, *Phys. Rev.* **D27** (1983) 552; *Phys. Rev.* **D29** (1984) 75.
- [29] M.C. Noecker, B.P. Masterson and C.E. Wieman, *Phys. Rev. Lett.* **61** (1988) 310.
- [30] C.S. Wood *et al.* , *Science* **275** (1997) 1759.
- [31] G.L. Fogli and D. Haidt, *Z. Phys.* **C40** (1988) 379
- [32] K. McFarland *et al.* , *Eur. Phys. J.* **C1** (1998) 509.
- [33] CHARM-II Collaboration, *Phys. Lett.* **B281** (1992) 159.
- [34] P. Janot, talk given at International Europhysics Conference on High Energy Physics, Jerusalem 1997.
- [35] G.L. Kane, C. Kolda and J.D. Wells, *Phys. Rev. Lett.* **70** (1993) 2686;
D. Comelli and C. Verzegnassi, *Phys. Lett.* **B303** (1993) 277.
- [36] M. Cvetič and P. Langacker, hep-ph/9707451, to appear in *Perspectives in Supersymmetry*, (ed.) G.L. Kane, World Scientific.
- [37] CDF Collaboration, *Phys. Rev. Lett.* **79** (1997) 2192.
- [38] Y. Umeda, G.C. Cho and K. Hagiwara, hep-ph/9805447.
- [39] M. Drees, N.K. Falck and M. Glück, *Phys. Lett.* **B167** (1986) 187.
- [40] K. Dienes, *Phys. Rep.* **287** (1997) 447.

- [41] M. Cvetič and S. Godfrey, summary of the Working Subgroup on Extra Gauge Bosons of the DPF long-range planning study, in *Electro-weak Symmetry Breaking and Beyond the Standard Model*, (ed). T. Barklow *et al.* , World Scientific (1995) (hep-ph/9504216).